universität wien

MASTERARBEIT / MASTER'S THESIS

Titel der Masterarbeit / Title of the Master's Thesis

„Analysis of *Arabidopsis thaliana* N-degron pathways with tandem fluorescent protein timer constructs“

verfasst von / submitted by

Jessica Böhm

angestrebter akademischer Grad / in partial fulfilment of the requirements for the degree of

Master of Science (MSc)

Wien, 2023 / Vienna, 2023

Studienkennzahl lt. Studienblatt / degree programme code as it appears on the student record sheet:	UA 066 877
Studienrichtung lt. Studienblatt / degree programme as it appears on the student record sheet:	Masterstudium Genetik und Entwicklungsbiologie
Betreut von / Supervisor:	Univ.-Prof. Mag. Dr. Andreas Bachmair

Acknowledgements

First, I would like to thank my supervisor Univ.-Prof. Mag. Dr. Andreas Bachmair for giving me the opportunity to work in his lab on this really interesting project. I am very thankful for his support, expertise, and patience during the whole process of creating this thesis.

Further, I would like to thank Lilian Nehlin, Jose Julian Valenzuela, Sadia Sabrina Alam, Bushra Ijaz and Bernhard Wurzinger for admitting me not only to the lab, but also to their lives. Special thanks go to Nikola Winter, for her excellent mentoring throughout the entire Master´s thesis and for sharing her practical experience. Thank you for guiding me through all the new, scientific and non-scientific, things I have learned during this thesis. You were amazing colleagues and I really enjoyed spending my time with you guys!

Finally, I would like to thank my parents, Helmut and Kathrin, my brother Tobias, and my additional family member Apollo, for their constant support and for teaching me all the lessons in life that helped me through all the years of my studies. Danke!

Table of Contents

I. Abstract

Plants as sessile organisms rely on rapid and precise protein degradation in response to stress and environmental changes. One way of regulating protein abundance is the N-degron pathway, which links the N-terminal amino acid of a protein to its half-life. To analyze the degradation of substrates by the plant E3 ligase of interest from this pathway, tandem fluorescent protein timer constructs with different N-terminal amino acids were co-expressed in yeast with defect in its endogenous N-degron pathway.

This work shows, that besides type I also type II N-degron constructs are substrates for PRT6 and that they share one interaction domain. Additionally, potential mutations to interrupt binding of hydrophobic N-degrons were identified.

Furthermore, it was shown that the potential N-recognin BIG indeed leads to degradation of substrates, when expressed in combination with UPL2 and UBC2. The mutation of UPL2´s cysteine (3625) to alanine led to a stabilization of the substrates and the assumption that the protein has a catalytic function in the system.

To enable the use of translation inhibitors for further experiments in yeast, a UBR1 deficient strain lacking the previously introduced KanMX cassette was developed.

On top of this, various N-degron substrates were transformed into *A. thaliana* plants and lines with single insertions, expressing the constructs were identified via Western blots. These plants can be used for microscopy approaches to determine subcellular localization and changes in degradation behavior depending on environmental influences, developmental stages, or treatment with diverse substances.

II. Zusammenfassung

Pflanzen als sessile Organismen sind auf den schnellen und präzisen Abbau von Proteinen als Reaktion auf Stress oder Umweltveränderungen angewiesen. Ein Weg, die Protein Abundanz zu regulieren, ist der „N-degron pathway“, der die N-terminale Aminosäure eines Proteins mit seiner Halbwertszeit verknüpft. Um den Abbau von Substraten durch die pflanzliche E3 Ligase von Interesse zu analysieren, wurden „tandem fluorescent timer protein“ Konstrukte mit unterschiedlichen N-terminalen Aminosäuren zusammen mit der Ligase in Hefezellen exprimiert, deren endogener N-degron pathway stillgelegt wurde.

Diese Arbeit zeigt, dass neben Typ I auch Typ II N-degron Konstrukte Substrate für PRT6 sind und sie sich eine Interaktionsdomäne teilen. Zusätzlich wurden potenzielle Mutationen zur Unterbrechung der Bindung hydrophober N-degrons identifiziert.

Außerdem wurde gezeigt, dass das potenzielle N-recognin BIG tatsächlich zum Abbau von Substraten führt, wenn es in Kombination mit UPL2 und UBC2 exprimiert wird. Die Mutation von UPL2s C3625 zu Alanin führte zur Stabilisierung der Substrate und der Annahme, dass das Protein eine katalytische Funktion in dem System hat.

Um den Gebrauch von Translationsinhibitoren für weitere Experimente in Hefe zu ermöglichen, wurde ein UBR1 defizienter Stamm ohne die vormals eingefügte KanMX Kassette entwickelt.

Darüber hinaus wurden diverse N-degron Substrate in *A. thaliana* Pflanzen transformiert und mittels Western Blot Linien mit einfacher Insertion identifiziert, die das Konstrukt exprimieren. Diese Pflanzen können für mikroskopische Analysen verwendet werden, um die subzelluläre Lokalisation und Unterschiede im Abbauverhalten abhängig von Umwelteinflüssen, Entwicklungsstadien oder Behandlung mit diversen Substanzen zu ermitteln.

Abbreviations

°C ..... *degree celsius*
µF ..... *microfarad*
µL ..... *micorliter*
µM ..... *micromolar*
A ..... *alanine*
aa ..... *amino acids*
ADH ..... *alcohol dehydrogenase*
Amp ..... *ampicillin*
ars ..... *autonomously replicating sequence*
Ca^{2+} ..... *calcium ion*
$CaCl_2$ x $2H_2O$ ..... *calcium chloride dihydrate*
Cap ..... *chloramphenicol*
cen ..... *centromeric region*
CHX ..... *cycloheximide*
CRISPR ..... *clustered regularly interspaced short palindromic repeats*
D ..... *aspartic acid*
DEPC ..... *diethy pyrocarbonate*
dH_2O ..... *deionized water*
DHFR ..... *dihydrofolate reductase*
DMSO ..... *dimethylsulfoxide*
E ..... *glutamic acid*
E.coli ..... *Escherichia coli*
EDTA ..... *ethylenediaminetetraacetic acid*
EM ..... *electron microscopy*
EMBL ..... *european molecular biology laboratory*
ER ..... *endoplasmatic reticulum*
F ..... *phenylalanine*
g ..... *gramm*
Genta ..... *gentamycin*
h ..... *hour*
H ..... *histidine*
HECT ..... *homologous to E6-AP C-terminus*
HEPES ..... 4-(2-hydroxyethyl)-1-piperazineethanesulfonic acid
His ..... *histidine*
HRP ..... *horseradish peroxidase*
Hyg ..... *hygromycin*
Ile ..... *isoleucine*
K ..... *lysine*
Kan ..... *kanamycin*
KCl ..... *potassium chloride*
KCMF1 ..... *potassium channel modulatory factor 1*
kDa ..... *kilo dalton*
KH_2PO_4 ..... *Monopotassium phosphate*
kV ..... *kilovolt*

L ..... *liter, leucine*
LB ..... *lysogeny broth*
Leu ..... *leucine*
LiAC ..... *lithium acetate*
M ..... *methionine*
mCherry ..... *red fluorescent protein*
MES ..... *2-(N-morpholino)ethanesulfonic acid*
$MgCl_2$ ..... *magnesium chloride*
$MgSO_4$ ..... *magnesium sulfate*
min ..... *minutes*
mL ..... *milli liter*
ML ..... *methionine leucine*
$MnCl_2$ x 4 H_2O ..... *mangandichloride tetrahydrate*
MS ..... Murashige and Skoog medium
Na_2HPO_4 ..... *disodium phosphate*
NaCl ..... *sodium chloride*
ng ..... *nanogramm*
OD_{600} ..... *optical density at 600nm*
ONP ..... *ortho-Nitrophenol*
ONPG ..... *ortho-Nitrophenyl-ß-galactoside*
PBS-T ..... *phosphate-buffered saline with Tween® detergent*
PEG ..... *polyethylene glycol*
pH ..... *potential of hydrogen*
PRT6 ..... *proteolysis6*
PTM ..... *post translational modification*
PVDF ..... *polyvinylidene difluoride*
R ..... *arginine*
RBR ..... *RING between RING*
Rif ..... *rifampicin*
RING ..... *really interesting new gene*
rpm ..... *revolutions per minute*
RT ..... *room temperature*
S ..... *serine*
SD ..... *synthetic defined*
sfGFP ..... *superfolder green fluorescent protein*
SOC ..... *super optimal broth with catabolite repression*
ssDNA ..... *single stranded deoxyribonucleic acid*
ß-Gal ..... *beta-galactosidase*
TE ..... *TRIS EDTA*
TFB ..... *transformation buffer*
tFT ..... *tandem fluorescent protein timer*
TRIS ..... *2-Amino-2-(hydroxymethyl)propane-1,3-diol*
Trp ..... *tryptophane*
ub ..... *ubiquitin*
UBA ..... *ubiquitin activating*
UBC ..... *ubiquitin conjugating*
UBR ..... *ubiquitin recognition*

UPL2 ..... *ubiquitin-protein ligase 2*
UPS ..... *ubiquitin-26S proteasome system*
Ura ..... *uracile*
V ..... *valine*
W ..... *tryptophane*
xg ..... *gravitational acceleration*
Y ..... *tyrosine*
YEp ..... *Yeast Episomal plasmids*
YPD ..... *yeast extract peptone dextrose*
Ω ..... *Ohm*

List of tables

List of figures

1 Introduction

1.1 The ubiquitin-26S proteasome system

Proper degradation of proteins is an essential process in cells. It maintains cellular physiology, communication, and defense. One way to regulate protein abundance is degradation via the ubiquitin-26S proteasome system (UPS) (Gibbs et al. 2014). It consists of a cascade of three major enzymes, an E1 for activation (UBA) of the ubiquitin molecule, an E2 conjugating enzyme (UBC) and an E3 ligase, which provides the target specificity of the system. A schematic depiction of this cascade is shown in Figure 1 with the five basic steps indicated with circles. First, the UBA activates the ubiquitin depending on ATP by forming a thioester bond. The ubiquitin is then transferred to a UBC by a transesterification reaction. In the third step, the ubiquitin can be bound covalently by the E3 for ligation to the target, or the ligase mediates the interaction between target and E2 enzyme. The different characteristics of these types of ligases will be explained in more detail below. The ubiquitinated substrate is then recognized and degraded by the proteasome concomitant with cleavage of the ubiquitin molecules by deubiquitylating enzymes and recycling.

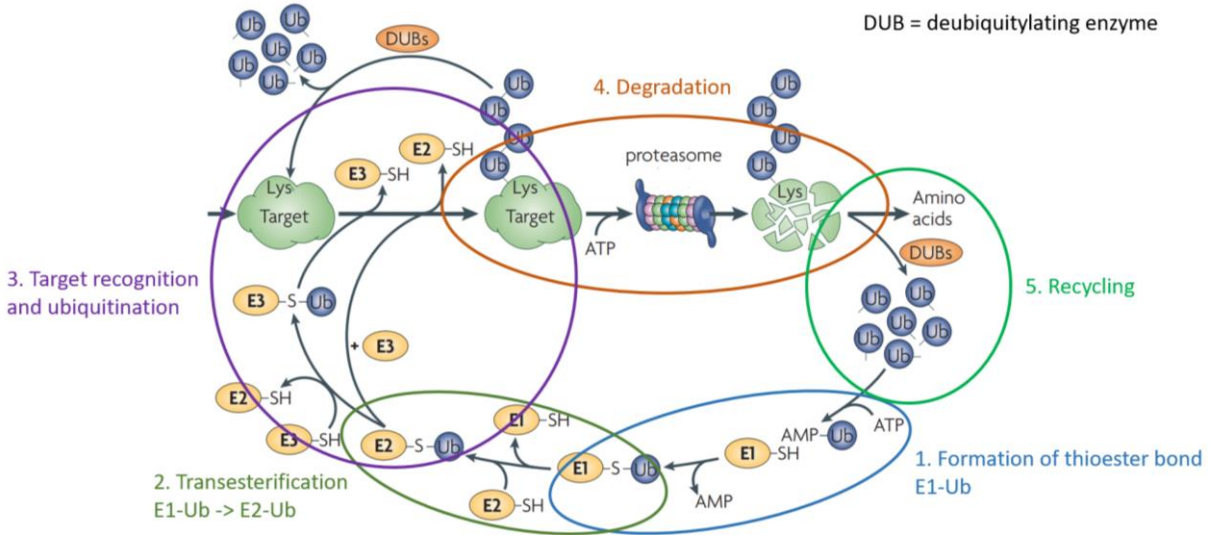

Figure 1: Basic steps of the ubiquitin-26S proteasome system degradation pathway
Figure modified from Vierstra 2009

One major branch of this system is the N-degron pathway, where substrates are recognized depending on their N-terminal amino acid as degradation signal (Mogk et al. 2007).

1.2 *The N-degron pathway*

Targets for this kind of degradation pathway need a flexible N-terminal extension, nearby lysin residues for ubiquitin binding, and an N-terminal amino acid that acts as degradation signal, named N-degron. Figure 2 shows different types of N-degrons in plants. There are, from left to right, primary (red, green and pink), secondary (blue) and tertiary (pink) N-terminal degradation signals, which require processing via several enzymatic reactions (Varshavsky 2011).

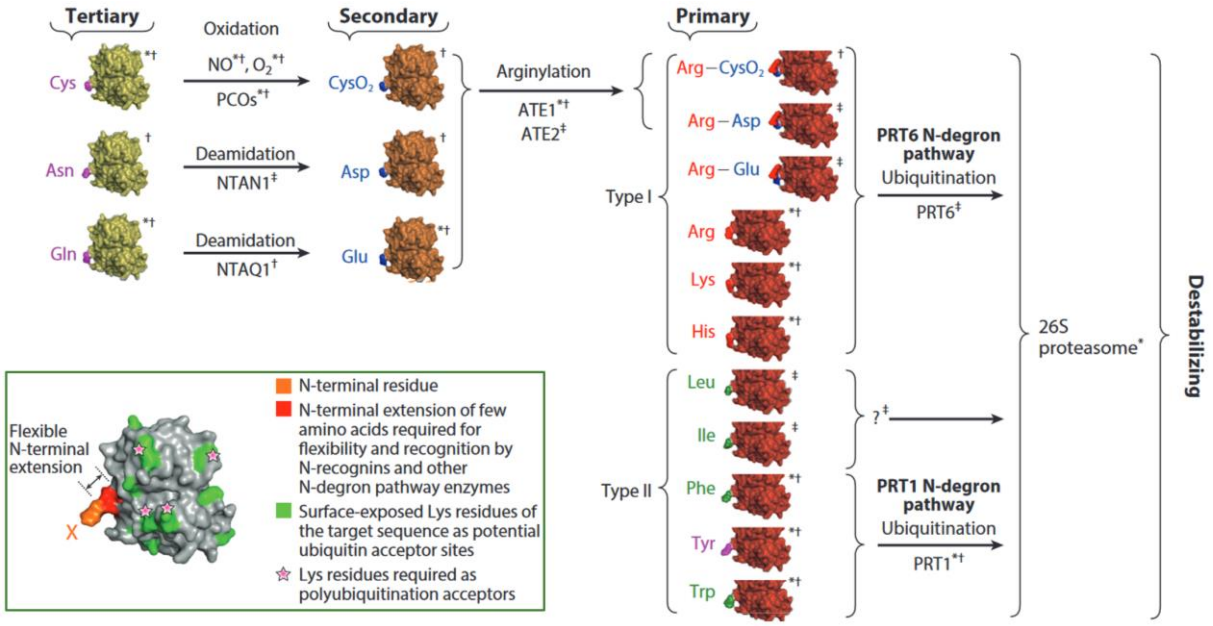

Figure 2: Different types of N-degrons in plants
Figure modified from Dissmeyer 2019

Prior to ubiquitylation, all N-degrons belong to the primary class and can be divided into two types. According to Dissmeyer 2019, type I, basic N-degrons interact with PRT6, and type II, hydrophobic N-terminal amino acids phenylalanine, tyrosine and tryptophane are recognized by PRT1, while the E3 ligase for degradation of leucine and isoleucine remains unclear.

As the pathway is conserved in all eukaryotes, and UBR1 is the only E3 ligase in *S. cerevisiae*, it is able to interact with both types of N-degrons. For this, it has two different domains, as shown in the cryo electron microscopy structure in Figure 3. Additionally to UBR1 in light grey, an E2 enzyme in yellow with the bound ubiquitin in orange are depicted. The two different substrate recognition sites are highlighted. UBR-box-1 for recognition of type I

N-degrons is indicated in pink, and the ClpS-like motif for interaction with type II substrates in blue. A more detailed depiction of these binding pockets is shown in sections A, UBR-box-1 with arginine-substrate and zinc ion for structural stabilization, and B, ClpS-like motif with phenylalanine-substrate.

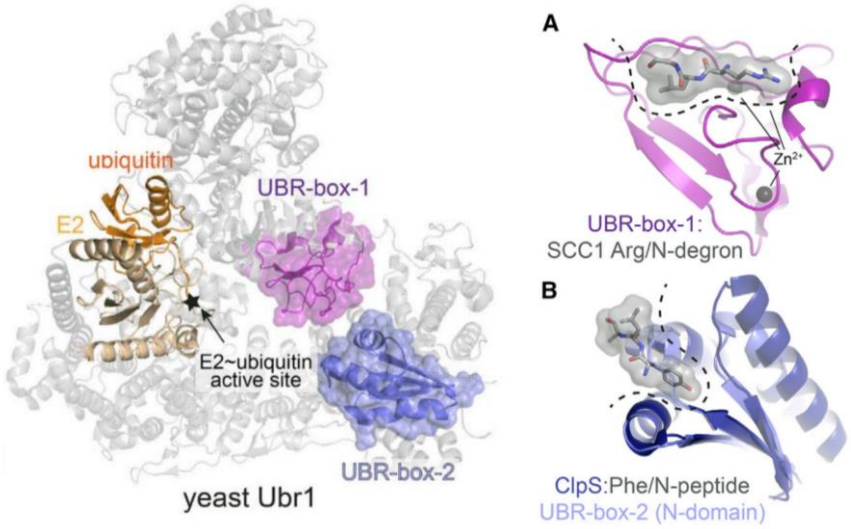

Figure 3: Cryo electron microscopy structure of yeast UBR1
Detailed depiction of substrate binding to UBR domain (A) and ClpS-like motif (B)
Figure modified from Sherpa et al. 2022

Besides different types of N-degrons and specific interaction sites, there are also various types of E3 ligases. As mentioned in the beginning, one can separate them into two categories. One that binds the ubiquitin molecule covalently prior to transfer to the substrate, named HECT E3 ligases and RBR E3 ligases, and another one which only mediates the interaction between ubiquitylated E2 and target, called RING E3 ligases. Structures of the specific domains from these E3 types are depicted in Figure 4.

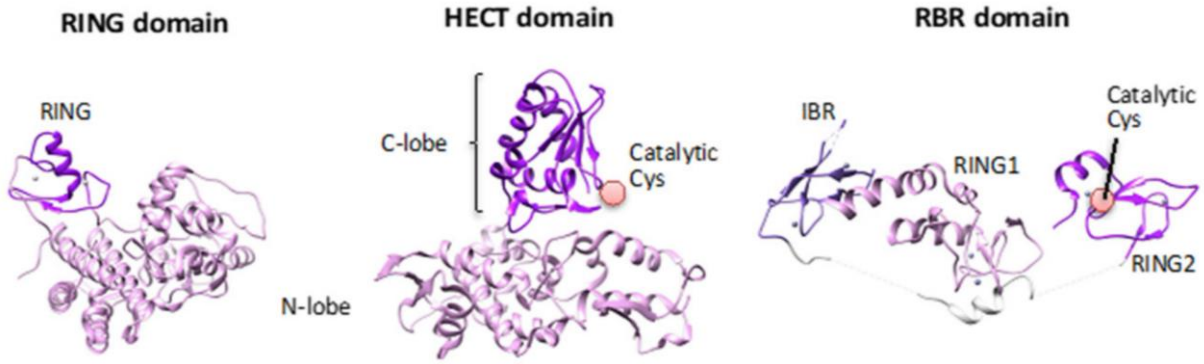

Figure 4: Structural depiction of E3 type interaction domains (Toma-Fukai and Shimizu 2021)

The RING domain shown on the left site without a catalytically active center, enables target ubiquitination by conformational changes of itself and the conjugating E2 enzyme (Zheng and Shabek 2017). This process depends on the availability of positively charged zinc ions. As this domain is the smallest and simplest of the three described types, it also has the most diverse range of activity. Some of the RING E3 ligases can act as monomers, while others need to form homodimers, or even need to build multi-subunit complexes with other proteins (Chen and Hellmann 2013).

Compared to this, HECT E3 ligases have a catalytically active cysteine in their C-terminal region for covalent binding of the ubiquitin molecule (C-lobe) and an E2 and target recognition domain at their N-terminal end (N-lobe). RBR domain E3 ligases act in a similar way. Here, the active cysteine for ubiquitin binding is part of the RING2 domain, and E2 or target interactions are accomplished by the RING1 domain (Kim et al. 2021; Pickart 2001).

1.3 Arabidopsis thaliana

Especially in plants as sessile organisms, rapid and accurate regulation of protein levels in response to stress or environmental changes is very important (Al-Saharin et al. 2022). One way to regulate protein levels are post translational modifications (PTMs; Millar et al. 2019), and one PTM is the ligation of ubiquitin molecules to targets and their subsequent degradation, as explained before.

Arabidopsis thaliana with its life-cycle of roughly 3 months, its well characterized genome, and a lot of known pheno- and genotypes, is the most common model organism for studying plant biology (Meinke et al. 1998). Studies of the last decades showed that the UPS has an important role in various stages of *A. thaliana* development, from germination to the timing of flowering, and in response to stresses such as drought or high salt concentrations (Shu and Yang 2017).

An important environmental change is the availability of oxygen for example during flood. The sensing of oxygen is a special part of the N-degron pathway in plants for targets with N-terminal cysteine, as shown in the first row of Figure 2. In this case, the cysteine is processed by different enzymes depending on the level of oxygen surrounding the plants, which leads to adjusted substrate half-life (Heo et al. 2021).

The three different, known, or potential N-recognins used for this work are listed below with their description and some characteristics from TAIR (www.arabidopsis.org).

1.3.1 PRT6

Described as component of the N-end rule pathway (Garzón et al. 2007) that targets protein degradation through the identity of the amino-terminal residue of specific protein substrates by TAIR (AT5G02310). Phylogenetic tree depicted in Figure 25.

Table 1: Abstract of PRT6 characteristics according to TAIR

Involved in biological processes	Protein ubiquitination Ubiquitin-dependent protein catabolic process via the N-end rule pahtway
Located in cellular components	Cytoplasm
Molecular functions	Ubiquitin protein ligase activity Ubiquitin-protein transferase activity Zinc ion binding

1.3.2 BIG

Described as calossin-like protein required for auxin transport by TAIR (AT3G02260). Phylogenetic tree depicted in Figure 26.

Table 2: Abstract of BIG characteristics according to TAIR

Involved in biological processes	Auxin polar transport Inflorescence morphogenesis Lateral root formation Response to fungus Unidimensional cell growth
Located in cellular components	Cytosol Plasmodesma
Molecular functions	Zinc ion binding

1.3.3 UPL2

Described as ubiquitin-protein ligase-like protein containing a HECT domain by TAIR (AT1G70320). Phylogenetic tree depicted in Figure 27.

Table 3: Abstract of UPL2 characteristics according to TAIR

Involved in biological processes	Protein poly-/ ubiquitination

Located in cellular components	Cytosol Mitochondrion Nucleus
Molecular functions	Ubiquitin protein ligase activity Ubiquitin-protein transferase activity

1.4 Reporter constructs

Reporter constructs used in the Bachmair lab to monitor protein stability have evolved from ß-galactosidase with different N-degrons as substrates (A) over test-proteins tagged with a green fluorescent protein (B) to tandem fluorescence protein timers (tFTs) containing mCherry and sfGFP (C), depicted in Figure 5.

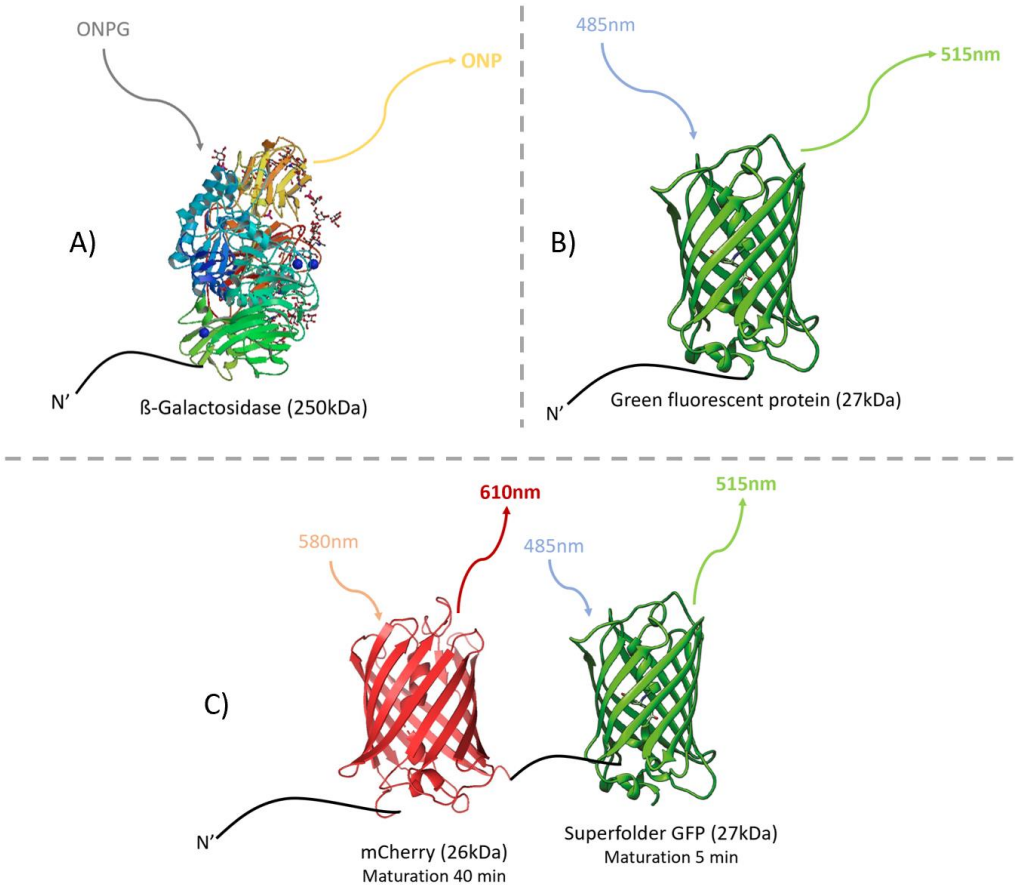

Figure 5: Different types of reporter constructs to detect protein stability

To detect the stability of different N-degrons with the ß-Gal constructs, one has to extract the proteins from the yeast cells and add ONPG as substrate for ß-galactosidase, that degrades it to ONP, which shows a yellow color. The more stable the construct, the higher the number of ß-galactosidase molecules for the reaction, and the darker the yellow color.

As the protein extract is needed for the reaction, it is not possible to measure the stability of N-degrons over time (Kozlic et al. 2021).

To overcome this problem, reporters tagged with a green fluorescent protein were introduced. In this system, the substrate, either a protein of interest or only a flexible linker with lysine residues as ubiquitin acceptation sites and different N-terminal amino acids, is fused to GFP. The substrate stability is then interpreted as the green fluorescence normalized to the optical density of the culture at 600nm. The excitation of GFP at 485nm leads to an emission of light with 515nm wavelength for detection. This causes no harm to the cells and offers the possibility to measure protein kinetics (Kozlic et al. 2021; Böhm et al. 2023).

This system was further improved by the invention of tandem fluorescent protein timers (Khmelinskii et al. 2012). Theses constructs contain besides sfGFP with a maturation time of about 5 minutes, additionally mCherry with a maturation time of around 40 minutes. This gives on one hand the opportunity to distinguish between unstable substrates, that are degraded in under 5min and do not show any fluorescence signal, stable substrates that are degraded earliest after 40min, where both fluorescence signals can be detected, and an intermediate type, where degradation takes place between 5 and 40 minutes, which leads to mostly green fluorescence of the cells. On the other hand, it is not only possible to interpret the stability of different N-degrons as green fluorescence per OD_{600}, but also as red per green fluorescence, which makes the system less open to influences such as different plasmid copy numbers or growth rate of the cells and environmental conditions (Böhm et al. 2023).

How these reporters are expressed in the cells, is shown in Figure 6. To generate the N-terminal amino acid of choice, the co-translational cleavage signal from ubiquitin (ub) is used (Bachmair et al. 1986). As the yeast strain CB80ΔUBR, used for experimental determination of stability of different N-degron substrates, lacks its only endogenous N-recognin UBR1, one can test the influence of E3 ligases of interest on substrate degradation by adding a plasmid for their expression to the system. This worked for PRT1, as published by Stary et al. 2003. In other cases, as for PRT6, a plant E2 conjugating enzyme, UBC2, was needed for the ligase to be active (Kozlic et al. 2021).

For yeast experiments in this work, the test protein consists of a flexible linker with lysine for ubiquitination and the N-terminal amino acid of choice, while the constructs transformed into plants, have the protein DHFR, an established substrate of the N-degron pathway in plants (Bachmair et al. 1986; Bachmair et al. 1993), as test protein.

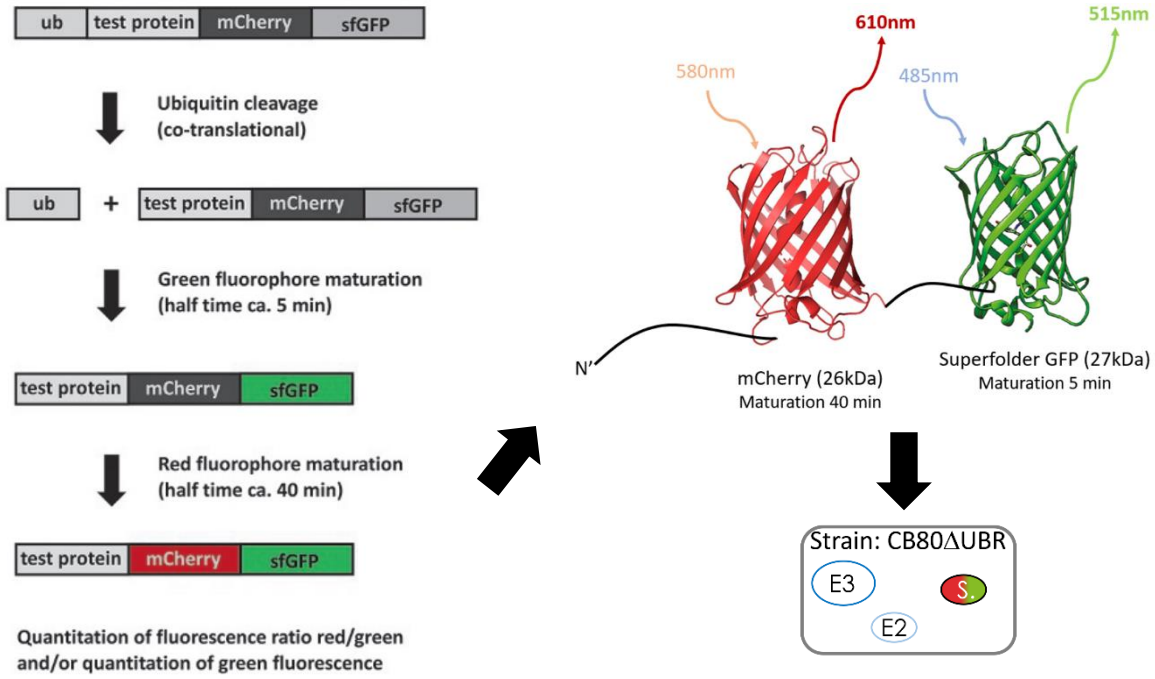

Figure 6: Schematic depiction of tFT expression
Figure modified from Kozlic et al. 2021 and Böhm et al. 2023

An additional tool to increase the differences in stability between various N-degron substrates is to inhibit translation at one point and measure the time, until they are completely or to 50% degraded. The KanMX cassette, introduced for selection into the CB80ΔUBR strain, makes the cells resistant to G-418 (Lorenz 2015) and the translation inhibitor cycloheximide, see Figure 9. Therefore, we developed the new CB80ΔUBR – KanMX strain, which should be sensitive to translation inhibition.

1.5 Aim of this work

Aim of this work was to further investigate PRT6 substrates and interaction domains, the functional reconstitution of the potential N-recognin BIG in yeast and the development of plant lines expressing different tFT reporter constructs for microscopy studies. Additionally, a UBR1 deficient yeast strain lacking the KanMX cassette was generated, to allow the use of translation inhibitors for further experiments.

2 Material and Methods

2.1 Material

2.1.1 Bacterial strains

The following table lists the bacterial strains used for this work.

Table 4: Bacterial strains used for this work

Organism	Strain	Selection
E. coli	DH5α	/
A. tumefaciens	GV3101	/

2.1.2 Yeast strains

The yeast strains used for this work are shown in the table below.

Table 5: Yeast strains used for this work

Organism	Strain	Selection
S. cerevisiae	CB80ΔUBR	G-418
S. cerevisiae	CB80ΔUBR - KanMX	/

2.1.3 Plant lines

For this work, the following plant lines were used.

Table 6: Plant lines used for this work

Organism	Line	Selection	Glycerolstock # *A. tumefaciens*
A. thaliana	Col 0	/	/
A. thaliana	Col 0 + R-tFT	Hyg	3335
A. thaliana	Col 0 + V-tFT	Hyg	3336
A. thaliana	Col 0 + M-tFT	Hyg	3546
A. thaliana	Col 0 + L-tFT	Hyg	3547
A. thaliana	Col 0 + F-tFT	Hyg	3548
A. thaliana	Col 0 + C-tFT	Hyg	3549
A. thaliana	Col 0 + D-tFT	Hyg	3550
N. benthamiana	/	/	/

2.1.4 Vectors and oligonucleotides

2.1.4.1 Vectors for yeast transformation

YCplac22:

The vector YCplac22 is an *E. coli* - yeast shuttle constructed by Gietz and Sugino 1988. It contains an ampicillin resistance gene for selection in *E. coli* and the *trp1* gene for selection and an ars-cen cassette for stable maintenance in yeast. For this work, it further contained the *prt6* or *big* gene as 3xHA-tagged or untagged versions, cloned by Winter, N., Nehlin, L. and Kozlic, A. Furthermore, the plasmids YCplac22-PRT6 and YCplac22-3xHA-PRT6 were modified with different point mutations by myself, as listed in Table 7.

Table 7: Constructs cloned into vector YCplac22

Construct	Yeast selection	Bacteria selection	Glycerolstock #
pAida_BIG classic	Trp	Amp	3266
pAida_BIG-3xHA-clean	Trp	Amp	3248
HA-PRT6	Trp	Amp	2779
PRT6_UBRmut	Trp	Amp	3664
PRT6	Trp	Amp	2631
3HA-PRT6mutAF	Trp	Amp	3728
3HA-PRT6mutAK	Trp	Amp	3729
3HA-PRT6mutAS	Trp	Amp	3730

pGADT7:

For this work, Winter, N. and Kozlic, A. cloned the gene encoding UPL2 under the control of the ADH1 promoter into the pGADT7 vector. It has an ampicillin resistance marker for selection in bacteria and a sequence to express leucine for selection in yeast. Additionally, I cloned a C to A point mutation myself into the existing plasmid. Constructs and glycerolstock numbers for this vector are shown in Table 8.

Table 8: Constructs cloned into vector pGADT7

Construct	Yeast selection	Bacteria selection	Glycerolstock #
UPL2	Leu	Amp	3411
UPL2mutCtoA	Leu	Amp	3756

pAG413GAL:

This vector contains chloramphenicol and ampicillin resistance genes and a histidine marker for selection in bacteria and yeast. For this work, sequences encoding the plant E2 enzymes UBC2 and UBC3 were cloned into the plasmid by Winter, N. and replaced the chloramphenicol resistance gene. The constructs are listed in Table 9 and express the proteins under the control of a galactose promoter.

Table 9: Constructs cloned into vector pAG413Gal-ccdB

Construct	Yeast selection	Bacteria selection	Glycerolstock #
UBC2	His	Amp	2764
UBC3	His	Amp	2766

YEplac195:

For cloning the substrates with different N-degrons, again under the control of a galactose promoter, the vector YEpURAubAD was used by Winter, N. It contains an ampicillin resistance and a uracil marker for selection, as shown in Table 10.

Table 10: Constructs cloned into vector YEplac195

Construct	Yeast selection	Bacteria selection	Glycerolstock #
V-lacI-KtFT	Ura	Amp	3433
R-lacI-KtFT	Ura	Amp	3434
A-lacI-KtFT	Ura	Amp	3439
D-lacI-KtFT	Ura	Amp	3440
F-lacI-KtFT	Ura	Amp	3441
H-lacI-KtFT	Ura	Amp	3442
K-lacI-KtFT	Ura	Amp	3443
ML-lacI-KtFT	Ura	Amp	3444
S-lacI-KtFT	Ura	Amp	3445
L-lacI-KtFT	Ura	Amp	3446
Tyr-KnoptFT	Ura	Amp	3480
Trp-KnoptFT	Ura	Amp	3482
Ile-KnoptFT	Ura	Amp	3487
Met-KnoptFT	Ura	Amp	3488

2.1.4.2 Vectors for plant infiltration and transformation

pBIB-Hyg:

For infiltration and transformation of the plant lines, agrobacteria carrying tFT constructs cloned into the vector pBIB-Hyg were used. For selection in the different organisms, it contains kanamycin (in bacteria) and hygromycin (in plants) resistance markers and additionally genes for integration to the plant genome. The cloning was done by Sandbohr, J., Winter, N., and myself for this work, and constructs are listed in Table 11.

Table 11: Constructs cloned into vector pBIB-Hyg

Construct	Plant selection	Bacteria selection	Glycerolstock #
V-tFT 5th generation	Hyg	Kan, Rif, Genta	3274
R-tFT 5thGen	Hyg	Kan, Rif, Genta	3254
G5-M-tFTsfGFP2	Hyg	Kan, Rif, Genta	3504
G5-L-tFTsfGFP2	Hyg	Kan, Rif, Genta	3505
G5-F-tFTsfGFP2	Hyg	Kan, Rif, Genta	3506
G5-C-tFTsfGFP2	Hyg	Kan, Rif, Genta	3507
G5-D-tFTsfGFP2	Hyg	Kan, Rif, Genta	3514

2.1.4.3 Oligonucleotides

Oligonucleotides used for this work are listed in Table 30 and were ordered from Microsynth AG (Balgach, Switzerland).

2.1.5 Buffer, Media, and Antibiotics

The following tables show the used buffer, media, stocks, and antibiotics for the different parts of this work.

2.1.5.1 Bacteria

Table 12: General media and stock solutions for bacteria

SOC	2% Tryptone 0.5% Yeast extract 10mM NaCl 2.5mM KCl 10mM $MgCl_2$ 10mM $MgSO_4$ 20mM Glucose
LB	10g Tryptone

	5g Yeast extract 10g NaCl (15g Agar) Fill up to 1L with MilliQ H_2O Autoclave at 121°C, 20min, 1 bar above sea level
2xTY	16g Tryptone 10g Yeast extract 5g NaCl Fill up to 1L with MilliQ H_2O Autoclave at 121°C, 20min, 1 bar above sea level
SOB	20g Bacto Tryptone 5g Bacto Yeast extract 0.5844g NaCl 0.188g KCl To pH 6.8 – 7 Fill up to 1L with MilliQ H_2O Autoclave at 121°C, 20min, 1 bar above sea level
SOB complete	245mL SOB 2.5mL $MgCl_2$ (1M) 2.5mL $MgSO_4$ (1M)
TFB	0.605g Pipes 0.441g $CaCl_2$ x $2H_2O$ 3.728g KCl To pH 6.7 2.18g $MnCl_2$ x 4 H_2O Fill up to 200mL with MilliQ H_2O Filter sterilize 0.2µm Store at 4°C
1M MES pH 5.5	19.52g MES With KOH to pH 5.5 Fill up to 100mL with MilliQ H_2O Filter sterilize 0.2µm
1M $MgSO_4$	12.04g $MgSO_4$ Fill up to 100mL with MilliQ H_2O
100mM Acetosyringone	19.62g Acetosyringone Fill up to 10mL with ethanol
Infiltration medium	1mL 1M MES 1mL 1M $MgSO_4$ 150µL 100mM Acetosyringone Fill up to 100mL with autoclaved dH_2O

Table 13: Antibiotic stock solutions bacteria

Ampicillin	100mg/mL H_2O Filter sterilize 0.2µm
Gentamycin	50mg/mL H_2O

	Filter sterilize 0.2µm
Kanamycin	50mg/mL H_2O Filter sterilize 0.2µm
Rifampicin	50mg/mL DMSO Filter sterilize 0.2µm

2.1.5.2 Yeast

Table 14: General yeast media and stock solutions

10x DropOutMix (solid)	L-Alanine 2.0 g L-Lysine 2.0 g L-Arginine 2.0 g L-Methionine 2.0 g L-Asparagine 2.0 g para-Aminobenzoic acid 2.0 g L-Aspartic acid 2.0 g L-Phenylalanine 2.0 g L-Cysteine 2.0 g L-Proline 2.0 g L-Glutamine 2.0 g L-Serine 2.0 g L-Glutamic acid 2.0 g L-Threonine 2.0 g L-Glycine 2.0 g myo-Inositol 2.0 g L-Isoleucine 2.0 g L-Valine 2.0 g
10x DropOutMix (liquid)	10g (10x) DropOutMix (solid) Fill up to 500mL with MilliQ H_2O Filtrated: 0.45µm
SD medium -aa -sugar (0.8L)	1.9g Yeast Nitrogen Base (without amino acids and $(NH_4)_2SO_4$) 5.0g Ammonium sulfate (20g Agar) Fill up to 0.8L with MilliQ H_2O Autoclave at 121°C, 20min, 1 bar above sea level
YPD medium	10g Yeast extract 20g Peptone 20g Glucose (20g Agar) Fill up to 1L with MilliQ H_2O Autoclave at 121°C, 20min, 1 bar above sea level
20% galactose	100g galactose Fill up to 500mL with MilliQ H_2O Filtrated: 0.45µm

40% glucose	200g glucose Fill up to 500mL with MilliQ H_2O Filtrated: 0.45µm
20mL/l Ade	400mg adenosine Fill up to 100mL with MilliQ H_2O Filtrated: 0.45µm
100x Tyr	1.1g tyrosine Fill up to 200mL with MilliQ H_2O Filtrated: 0.45µm
2mL/L Leu	3g leucine Fill up to 200mL with MilliQ H_2O Filtrated: 0.45µm
100x His	0.6g histidine Fill up to 250mL with MilliQ H_2O Filtrated: 0.45µm
50x Ura	Provided by Telser, T.

Table 15: Antibiotic stock solutions yeast

Cycloheximide	1mg/mL and 10mg/mL DMSO
Nourseothricin	100mg/mL H_2O Filter sterilize 0.2µm

Table 16: Media and buffer for yeast transformations

SD + 2% glucose -Trp	100mL (10x) DropOutMix 50mL (40%) glucose 20mL (20mL/L) Ade 10mL (100x) Tyr 2mL (2mL/L) Leu 10mL (100x) His 20mL (50x) Ura (20g Agar) Fill up to 1L with SD -aa -sugar
SD + 2% glucose -Trp -His	100mL (10x) DropOutMix 50mL (40%) glucose 20mL (20mL/L) Ade 10mL (100x) Tyr 2mL (2mL/L) Leu 20mL (50x) Ura (20g Agar) Fill up to 1L with SD -aa -sugar
SD + 2% glucose -Trp -Leu	100mL (10x) DropOutMix 50mL (40%) glucose

	20mL (20mL/L) Ade 10mL (100x) Tyr 10mL (100x) His 20mL (50x) Ura (20g Agar) Fill up to 1L with SD -aa -sugar
SD + 2% glucose -Trp -His -Ura	100mL (10x) DropOutMix 50mL (40%) glucose 20mL (20mL/L) Ade 10mL (100x) Tyr 2mL (2mL/L) Leu 20g Agar Fill up to 1L with SD -aa -sugar
SD + 2% glucose -Trp -Leu -Ura	100mL (10x) DropOutMix 50mL (40%) glucose 20mL (20mL/L) Ade 10mL (100x) Tyr 10mL (100x) His 20g Agar Fill up to 1L with SD -aa -sugar
10x TE buffer	0.1M Tris-HCl 10mM EDTA To pH 7.5
TE/LiAc buffer	0.1M LiAc 1x TE buffer
MasterMix yeast transformation	60µL 10x TE buffer 60µL 1M LiAc 10µL ssDNA 470µL 50% PEG 3500

Table 17: Media for fluorescence assay

SD + 2% galactose + 0,1% glucose -Trp -His - Ura	100mL (10x) DropOutMix 100mL (20%) galactose 2.5mL (40%) glucose 20mL (20mL/L) Ade 10mL (100x) Tyr 2mL (2mL/L) Leu Fill up to 1L with SD -aa -sugar
SD + 2% galactose -Trp -His - Ura	100mL (10x) DropOutMix 100mL (20%) galactose 20mL (20mL/L) Ade 10mL (100x) Tyr 2mL (2mL/L) Leu Fill up to 1L with SD -aa -sugar
SD + 2% galactose + 0,1%	100mL (10x) DropOutMix

glucose -Trp -Leu - Ura	100mL (20%) galactose 2.5mL (40%) glucose 20mL (20mL/L) Ade 10mL (100x) Tyr 10mL (100x) His Fill up to 1L with SD -aa -sugar
SD + 2% galactose -Trp -Leu - Ura	100mL (10x) DropOutMix 100mL (20%) galactose 20mL (20mL/L) Ade 10mL (100x) Tyr 10mL (100x) His Fill up to 1L with SD -aa -sugar

2.1.5.3 Plants

Table 18: General plant media and buffer

MS	4.4g MS salts incl. Nitsch vitamins 10g Sucrose 0.5g MES 1M KOH to pH 5.7 3g Gelrite Fill up to 1L with Milli H_2O Autoclave at 121°C, 12min, 1 bar above sea level
Protein extraction buffer	450µL 1M HEPES pH 7.5 2000µL 10% SDS 150µL 1M DTT 100µL 1mg/mL Pepstatin 50µL Plant Protease Inhibitor Cocktail (Sigma, USA) 2250µL H_2O

Table 19: SDS-PAGE and Western Blot buffer

10x PBS	27mM KCl 1.37M NaCl 100mM Na_2HPO_4 20mM KH_2PO_4 pH 7.2 – 7.6
4x sample loading buffer	50mM Tis pH6.8 12.5mM EDTA 2% SDS 10% glycerol 1% ß-mercaptoethanol 0.02% Bromophenol Blue
5x SDS-PAGE running buffer	1M Glycine

	125mM Tris 0.5% SDS
1x PBS-T	0.05% Tween-20 to 1xPBS
1x Transfer buffer	190mM Glycine 25mM Tris 0.05% SDS 20% ethanol

Table 20: Antibiotic stock solutions plants

Cefotaxime	250mg/mL H_2O Filter sterilize 0.2µm
Hygromycin	50mg/mL H_2O Filter sterilize 0.2µm
Vancomycin	100mg/mL H_2O Filter sterilize 0.2µm

2.2 Methods

2.2.1 General methods

2.2.1.1 Polymerase Chain reaction (PCR)

Table 21 and Table 22 below list the composition and standard thermal cycling conditions for the Q5 Hight Fidelity DNA Polymerase from New England Biolabs (NEB, USA). This polymerase was due to its 3´ → 5´ exonuclease activity and its proofreading used for amplification of inserts for cloning.

Table 21: Composition of Q5 High Fidelity DNA Polymerase PCR reactions for a final volume of 100µl

Components	**Volume (µL)**
DNA template (1pg-10ng)	0.1
Q5 ® reaction buffer (5x)	20
dNTPs (2mM)	10
5´primer (100µM)	0.5
3´primer (100µM)	0.5
Q5 High Fidelity DNA Polymerase (2u/µl)	1
H2O	67.9
Total	100

Table 22: Q5 High Fidelity DNA Polymerase standard thermal cycling conditions

Step		Temperatur	Time
Initial denaturation		98°C	30''
Denaturation	35x	98°C	10''
Annealing		Primer specific	30''
Elongation		72°C	Product specific
Extension		72°C	5'

The following Table 23 and Table 24 list the composition and standard thermal cycling conditions for the GoTaq® (Promega, USA) DNA polymerase, which was used for amplification of fragments for sanger sequencing, quality control and colony PCRs.

Table 23: Composition of GoTaq® DNA Polymerase PCR reactions for a final volume of 25µl

Components	Volume (µL)
DNA template	1
Green GoTaq® reaction buffer (5x)	5
dNTPs (2mM)	2.5
5´primer (10µM)	1
3´primer (10µM)	1
GoTaq® DNA polymerase (5u/µl)	0.1
H2O	14.4
Total	25

Table 24: GoTaq® DNA Polymerase standard thermal cycling conditions

Step		Temperatur	Time
Initial denaturation		94°C	120''
Denaturation	35x	94°C	30''
Annealing		Primer specific	30''
Elongation		72°C	Product specific
Extension		72°C	5'

The primer specific melting temperatures were calculated with the NEB T_M calculator. The temperatures for amplifying the inserts for cloning are listed in Table 32. The elongation time is calculated depending on the length of the product with roughly 60sec per 1kb.

2.2.1.2 Restriction digest

The composition of the reaction for restriction digest of a plasmid for cloning is listed in Table 25. The used restriction enzymes are unique cutters and listed in Table 31. The buffer and temperature were selected with the NEBcloner® tool from New England Biolabs. The reactions were incubated for at least 3 hours.

Table 25: Composition of vector preparative restriction digest for cloning

Components	**Volume (µL)**
DNA template (7µg)	X
reaction buffer (10x)	15.0
Restriction enzyme1	7.0
Restriction enzyme2	7.0
H_2O	121 - X
Total	150

For controlling a cloned plasmids integrity, a reaction with a restriction enzyme that cuts 3-4 times was set up as shown in Table 26. Buffer and temperature were selected with the NEBcloner® tool and the reaction was incubated for at least 3 hours. The fragment pattern was analyzed with a 1.2% Agarose gel.

Table 26: Composition of vector diagnostic digest

Components	**Volume (µL)**
DNA template (500ng)	X
reaction buffer (10x)	2.5
Restriction enzyme	0.3
H_2O	22.2 - X
Total	25

2.2.1.3 Agarose gel electrophoresis

For Agarose gel electrophoresis, a 1.2% solution of Agarose in 1xTBE buffer (6g in 500mL) was used and stored at 50°C. Right before use, 4µL of Midori Green (BioZyme Scientific GmbH, Germany) per 100mL 1.2% Agarose gel solution is added for staining the DNA. After pouring the Gel, it solidifies in about 30 minutes and is transferred into a running box containing 1xTBE buffer. Depending on the application, different volumes of the samples were loaded to the gel. For the linearized vectors and amplified inserts for cloning for

example, the complete volume was loaded to separate them from unwanted fragments. For size comparison, 4µL of the GeneRuler™ 1kb Plus DNA Ladder (Thermo Scientific GmbH, Germany) was loaded. The Gel ran around one hour at 100V. Images were made with a ChemiDoc (Bio-Rad Laboratories, USA) using the ethidium bromide settings. Bands with the right size were cut from the gel and purified with the Wizard® SV Gel and PCR Clean-Up System from Promega (USA) before cloning or sequencing.

2.2.1.4 In-Fusion cloning

The In-Fusion cloning method enables seamless fusion of multiple DNA fragments with at least 15 bp overlapping sequences at the end. It uses the 3´ → 5´ exonuclease activity of a poxvirus DNA polymerase. The exposed overlapping single stranded ends can then spontaneously anneal. These metastable constructs are then transformed into *Escherichia coli*, where the endogenous polymerase repairs any left gaps (Zhu et al. 2007).

The kit from Takara (France) contains a In-Fusion® Snap Assembly Mastermix, in Table 28 called In-Fusion HD Enzyme. It is mixed with purified PCR amplified inserts and a digested backbone, according to 2.2.1.3 Agarose gel electrophoresis, 2.2.1.1 Polymerase Chain reaction (PCR) and 2.2.1.2 Restriction digest. The weight of the different components depends on their size, see Table 27.

Table 27: Size to weight tables for vector and inserts

Vector size	Weight to use
<10 kb	50- 100 ng
>10 kb	50- 200 ng

Insert size	Weight to use
<0.5 kb	10 - 50 ng
0.5 - 10 kb	50 - 100 ng
>10 kb	50 - 200 ng

Table 28: Composition of In-Fusion reaction

Component	Length (bp)	Ratio	Weight to use (ng)	Concentration (ng/µL)	Volume (µL)
InsertA (PCR Fragment)	A	2 - 5	$D = \frac{F * Ratio}{C/A}$	X	D/X
InsertB (PCR Fragment)	B	2 - 5	$E = \frac{F * Ratio}{C/B}$	Y	E/Y
Vector (digested plasmid)	C	1	F (from Table 27)	Z	F/Z
In-Fusion HD Enzyme	/	/	/	/	1
H_2O	/	/	/	/	Up to 5
Total					5

Based on this, one can adjust the ratio of vector to inserts in Table 28, which shows the calculations for the composition of the In-Fusion reaction. The reaction is incubated for 15 minutes at 50°C in a heating block, prior to heat-shock transformation to *Escherichia coli*.

2.2.1.5 Sequencing

Samples amplified by PCR were purified using the Wizard® SV Gel and PCR Clean-Up System and sent for Sanger sequencing to Microsynth AG (Vienna, Austria), while plasmids were purified with the Wizard® Plus SV Miniprep DNA Purification system and sent to plasmidsaurus (Eugene, Oregon, USA) for whole plasmid sequencing. DNA and oligos were prepared according to the companies' guidelines.

2.2.1.6 Seed sterilization

Approximately 50µl seeds were sterilized by adding 200µl DanKlorix and 800µl 96% Ethanol. This solution was shaken for 10 minutes. Following that, the seeds were washed three times with 1mL 96% Ethanol and subsequently dried on a Whatman filter paper sterilized with 70% Ethanol.

2.2.1.7 SDS-PAGE

The Gels were prepared according to Table 29 at least 30 minutes prior to use. The extracted protein samples were heated for 5 minutes at 95°C with 5x sample loading buffer before loading. For size comparison, 6µL of the PageRuler™ Plus Prestained Protein Ladder (Thermo Scientific™, Germany) were loaded. The gel ran in 1x SDS Running Buffer with 0.25A for around 45 minutes until the blue color from the loading buffer reached the bottom.

Table 29: Composition of a 12% Sodium dodecyl sulfate polyacrylamide gel

	Stacking Gel	**12% Resolving Gel**
Components	Volume (µL)	Volume (µL)
Acrylamide (30%)	330	2000
Tris-Cl pH 6.8 (1M)	250	/
Tris-Cl pH 8.8 (1M)	/	1950
SDS (10%)	20	50
Bromophenol Blue	20	/
APS (10%)	20	50
TEMED	2	4
H_2O	1358	946
Total	2000	5000

2.2.1.8 Western Blot

For blotting the size fractionated proteins from the polyacrylamide gel (see 2.2.1.7 SDS-PAGE) to a PVDF membrane, western blot sandwiches were assembled. Therefore, the membrane was wetted in 96% ethanol and then, next to the gel, equilibrated for 10 minutes by shaking in 1x transfer buffer. The proteins were transferred via wet blotting at 4°C for 30 minutes with 250V per sandwich. For verifying the protein transfer to the membrane, a Ponceau stain was done after opening the sandwiches and washing the membrane twice with dH_2O. For staining, the membranes were incubated 10 minutes in 50mL Ponceau staining solution. Subsequently after staining, they were rinsed two times in dH_2O and once in 96% ethanol for faster drying. Imaging was done with the colorimetric settings of a ChemiDoc. Afterwards, the membranes were activated in 96% ethanol and washed three times for 5 minutes in 25mL PBS-T prior to blocking in 10mL PBS-T 5% milk for 30 minutes by shaking at RT. Following this, the membranes were incubated in 5mL primary antibody solution, 1:1000 Anti-GFP IgG1, clones 7.1 and 13.1, from mouse (Roche, Germany) in PBS-T 5% milk, overnight at 4°C. Next, the membranes were washed 3 times for 5 minutes in 25mL PBS-T on a shaking platform and then incubated for two hours at RT with 10mL secondary antibody solution, 1:10000 Anti-mouse-HRP (GE Healthcare NA 931) in PBS-T 5% milk. Finally, before imaging, the membranes were washed 3 x 5 minutes in PBS-T and 2 x 5 minutes in PBS. Imaging was done after adding WesternBright Sirius HRP substrate solution (Advansta, USA) to the membrane with the colorimetric settings for the marker bands and chemiluminescent settings for detection of selected proteins.

2.2.2 Work with *Escherichia coli* (DH5α)

2.2.2.1 Preparation of competent cells

To make sure that the cells were as fresh as possible, some competent cells from -80°C were steaked out on a new LB-agar plate and grown overnight at 37°C. One of the colonies was then used to inoculate 250mL SOB medium. This culture grew roughly 16 hours at 37°C and 200rpm shaking to an OD_{600} between 0.45 and 0.75 before they were transferred to ice cold 50mL tubes and incubated for 10 minutes. The cells were harvested by centrifugation at 1000xg and 4°C for 10min. After removing the medium, 50mL TFB were used to resuspend the cells in each tube, before repeating the incubation and centrifugation steps. Afterwards,

the buffer was completely removed, and the cells were pooled carefully in 20mL TFB. After adding 1.5mL DMSO, the cells were incubated for 10 minutes on ice. This solution was aliquoted in 200µL to cold 1.5mL tubes and immediately frozen in liquid nitrogen before putting them to -80°C for long term storage. Quality of the chemically competent cells was tested by transforming them with 100ng of plasmid DNA and putting the cells in different dilutions to selective LB-agar plates. With the number of grown colonies on the next day, the transformation efficiency could be calculated. As control for possible contaminations, the transformation procedure was done with pure water instead of plasmid solution, and the cells were put on different selective LB-agar plates and should not grow.

2.2.2.2 Transformation

For transformation, 200µL of competent *E.coli* cells were carefully thawed on ice and added to the In-Fusion reaction, see 2.2.2.1 Preparation of competent cells and 2.2.1.4 In-Fusion cloning, and heat-shocked for 1 minute at 42°C. Subsequently, they were chilled for 2 minutes on ice before adding 800µL SOC medium and incubation for 1 hour at 37°C and 650rpm shaking. Afterwards, the cells were pelleted for 3 min with 3000rpm at RT, the supernatant was removed, and the cells were resuspended in the remaining liquid and plated with glass beads onto selective antibiotic LB-agar plates and grown overnight at 37°C.

2.2.2.3 Colony PCR

If colonies grow on the selective LB-agar plates, see 2.2.2.2 Transformation, they had been successfully transformed. To make sure that not only a re-ligated vector or a vector containing just one of maybe several inserts entered the cells, colony PCRs were performed. Therefore, a few cells from the colony were resuspended in 100µL DEPC H_2O and lysed for 10 minutes at 95°C in a PCR block. 1µL of this solution was then used as template for a PCR reaction, as described in Table 23 and Table 24. Primers for these reactions bind at the border sites of the new constructs, one at the backbone and the other one at the insert. The size of the amplified products was checked on an agarose gel.

2.2.2.4 Plasmid preparation and restriction digest

Colonies that showed positive results for the colony PCRs were chosen to inoculate 10mL selective LB medium and grown overnight at 37°C. The plasmids were purified using the

Wizard® Plus SV Minipreps DNA Purification System (Promega, USA) and further verified with a restriction digest as described in Table 26. The specific restriction pattern was analyzed via an agarose gel. Plasmids with the right pattern were sent for whole plasmid sequencing to plasmidsaurus or PCR fragments over the whole inserts were amplified and sent for Sanger sequencing to Microsynth AG.

2.2.3 Work with *Saccharomyces cerevisiae* (CB80ΔUBR)

2.2.3.1 Transformation

Plasmids were transformed into yeast cells based on the Lithium Acetate/Single-Stranded Carrier DNA/Polyethylene Glycol method described by Gietz and Woods 2002. For two transformations, a single colony was resuspended in 10mL selective SD medium and grown overnight at 30°C and 200rpm shaking. This culture was used to inoculate a main culture of 40mL YPD medium to a start OD_{600} of 0.25, which then grew at 30°C and 200rpm shaking up to an OD_{600} of 0.5 before being harvested by 2000xg centrifugation for 2 minutes. The supernatant was removed, and the pellet resuspended in 20mL 1xTE buffer. After repeating the centrifugation, the cells were resuspended in 200µL 1xTE/1xLiAC solution before adding them to 1200µL MasterMix containing additionally PEG and ssDNA (boiled at 95°C for 5min). This solution was shaken on a Vortex mixer for around 30 seconds. A fresh 2mL tube with 100ng plasmid in 20µL dH_2O was prepared, 700µL of the cell-MasterMix solution were added and incubated for 30 minutes at 30°C and 650rpm shaking. Afterwards, 70µL DMSO were added, the tubes gently inverted, and the cells heat shocked for 12 minutes at 42°C for uptake of the plasmid by the yeast cells. Next, they were chilled for 2min on ice prior to centrifugation at 2000rpm and RT for 1min. After discarding the supernatant, 500µL 1xTE were added, the cells resuspended for washing, and the centrifugation was repeated. In a final step, the supernatant was poured off, the pellet resuspended in 500µL (for small plasmids) or 100µL (for big plasmids) 1xTE buffer, 100µL plated with glass beads on selective SD-agar plates and grown at 30°C for at least 2 days.

2.2.3.2 DNA preparation

If huge plasmids were transformed, the integrity had to be controlled. Therefore, the DNA was extracted and PCR fragments across the whole coding sequence were amplified and analyzed on an agarose gel. To extract the DNA form yeast, a colony was resuspended in

100µL 20mM LiAc 1% SDS solution, mixed on a Vortex mixer, and incubated for 5min at 70°C. Next, 300µL 96% ethanol were added, the tube briefly shaken on a Vortex mixer, and centrifuged at 15000xg for 3 minutes for pelleting the cells. The supernatant was discarded, the cells were resuspended in 500µL 70% ethanol, and pelleted again by centrifugation. This step was repeated with 500µL absolute ethanol, before drying the pellet for 10 minutes at RT by opening the tube. For PCR, the dried pellet was resuspended in 100µL dH_2O, incubated for 10 minutes at 55°C to dissolve the DNA, and centrifuged at 15000xg for 1 minute to separate cell fragments from DNA. The supernatant was transferred into a fresh tube, DNA concentration was measured by Nanodrop, and 1µL of this solution was used as template for PCRs.

2.2.3.3 Fluorescence assay

For testing the activity of E3 ligases in yeasts, tandem fluorescent protein timer reporter constructs with sfGFP and mCherry were used, described by Böhm et al. 2023, according to the method explained by Kozlic et al. 2021. Yeasts transformed with the plasmids for expression of the needed enzymes and substrates were grown on selective SD-agar plates at 30°C. Some colonies from these plates were used to inoculate 2mL pre cultures with selective SD medium containing 2% galactose and 0.1% glucose, for four biological replicates of the test substrates, three for the controls R- and V-tFT and one for the ß-Gal autofluorescence control. These cultures were grown over one or two nights depending on the cell's growth rate and used to inoculate main cultures, additionally in 4 technical replicates, into 96-well-plates to an OD_{600} of 0.3 in selective SD medium with 2% galactose as exclusive carbon source. From these plates, the values for OD_{600}, green, and red fluorescence were measured for 0, 2, 4 and 24 hours after inoculation. From this, the average and standard deviation, of the ratios from green fluorescence to OD_{600} and red to green fluorescence normalized to V-tFT, were calculated according to Equation 1 for data interpretation.

Equation 1: Formulae to calculate the specific ratios for green fluorescence to optical density and red to green fluorescence

$$actual\ OD_{600}(well\ x) = OD_{600}(well\ x) - Average(OD_{600}(medium\ only))$$

$$actual\ fluores._{green}\ (well\ x) = fluores._{green}\ (well\ x) - Average\left(fluores._{green}\ (ß - Gal)\right)$$

$$actual\ fluores._{red}\ (well\ x) = fluores._{red}\ (well\ x) - Average\left(fluores._{red}\ (ß - Gal)\right)$$

$$Normalized\ \frac{GFP}{OD_{600}}\ (well\ x) = \frac{actual\ fluores._{green}\ (well\ x)}{actual\ OD_{600}\ (well\ x)}$$

$$Normalized\ \frac{mCherry}{GFP}\ (well\ x) = \frac{actual\ fluores._{red}\ (well\ x)}{actual\ fluores._{green}\ (well\ x)}$$

$$\%\ Normalized\ \frac{GFP}{OD_{600}}\ (well\ x) = \frac{Normalized\ \frac{GFP}{OD_{600}}\ (well\ x) \times 100}{Average\left(Normalized\ \frac{GFP}{OD_{600}}\ (VtFT)\right)}$$

$$\%\ Normalized\ \frac{mCherry}{GFP}\ (well\ x) = \frac{Normalized\ \frac{mCherry}{GFP}\ (well\ x) \times 100}{Average\left(Normalized\ \frac{mCherry}{GFP}\ (VtFT)\right)}$$

An example for these calculations is shown in 5.3.1 of the appendix.

The following Figure 7 shows the pipetting scheme for these assays with indicated positive and negative control on the right side and samples for background subtractions on the left.

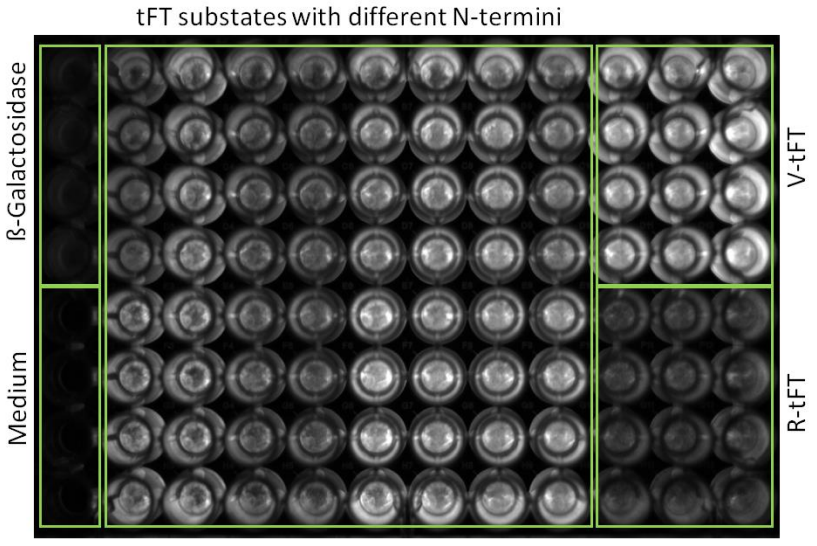

Figure 7: Pipetting scheme for tFT fluorescence assay: Upper left column, cells containing a ß-Galactosidase reporter construct to measure cell-autofluorescence; Lower left column, only medium to measure background absorption for correction of optical density; Upper right green box, stable control with cells expressing the V-tFT construct, later set to 100%; Lower right green box, cells with R-tFT construct as degradation control; Middle green box for test constructs with different N-termini

2.2.3.4 Development of a KanMX cassette deficient yeast CB80ΔUBR strain

To develop an *S. cerevisiae* strain lacking the UBR1 gene as well as the KanMX cassette for G418 resistance, the strain CB80ΔUBR, created by Telser, T., was transformed according to 2.2.3.1 with plasmid #3270, a yeast CRISPR vector (Generoso et al. 2016) containing a sequence for the KanMX cassette flanking regions, and additionally with the homologous, annealed oligos 3091 and 3232 as template for DNA repair via homologous recombination. Successfully transformed cells were selected with YPD+Nourseothricin-agar plates and grew for 2 days at 30°C. Colonies that lost their KanMX cassette were identified by putting them simultaneously with a toothpick on a YPD-agar plate and a YPD+G418-agar plate. Colonies that grew only on the non-selective plate lack the KanMX cassette. This procedure was repeated with these colonies on a YPD-agar plate and a YPD+Nourseothricin-agar plate to find cells that lost their KanMX cassette as well as the CRISPR vector.

2.2.4 Work with *Agrobacterium tumefaciens* (GV3101)

2.2.4.1 Transformation

For transforming *Agrobacterium tumefaciens*, around 200ng of prepared plasmid DNA and 100µL competent cells thawed on ice were added to a pre-cooled electroporation cuvette. The cells were shocked with 2.5kV, 25µF and 200Ω in the electroporator GenePulser®Bio-Rad. Afterwards, 950µL SOC medium was added to transfer the cells into a fresh tube and incubate them for 2h at 28°C and 700rpm shacking. 80µL were plated with glass beads on selective LB-agar plates and incubated at 30°C for growth.

2.2.5 Work with *Nicotiana benthamiana*

2.2.5.1 Leaf infiltration

To infiltrate leaves, a pre culture of 2mL selective LB medium inoculated with a single transformed colony of *A. tumefaciens* was grown overnight at 30°C and 200rpm shaking. A main culture of 20mL selective LB medium was inoculated with 200µL pre-culture and grown overnight at 30°C and 200rpm shaking. Cells were harvested for 20min at 2000xg and RT, resuspended in 20mL infiltration medium and kept longer than 1 hour at RT in darkness while gently shaking from time to time. OD_{600} was adjusted to 0.3 in a 2mL-tube and leaves

were infiltrated with a 5mL syringe without needle at the leaf's lowersurface of approximately 4 week old plants.

2.2.6 Work with *Arabidopsis thaliana*

2.2.6.1 Floral dipping

For transforming *A. thaliana*, roughly 6 week old plants are dipped into *A. tumefaciens* solutions. To obtain more flowers to be transformed, the main shoot was clipped off one week before floral dipping. For the dipping solution, pre cultures of 20mL selective 2xTY medium were inoculated from a single colony of transformed agrobacteria and grown overnight at 30°C and 200rpm shaking. For main culture, 2mL pre culture were used to inoculate 100mL selective 2xTY medium and grown overnight at 30°C and 200rpm shaking. Cells were harvested at 5000rpm and RT for 20 minutes and resuspended is 200mL 5% sucrose. Prior to 30 seconds of dipping, 40µL Silwet were added to the solution. Afterwards, the plants were covered with plastic bags and carried in a closed tray overnight. To enhance the efficiency of this method, the procedure was repeated one week after the first dipping. This protocol is based on a publication from Clough and Bent 1998.

2.2.6.2 Mendel segregation

After harvesting the seeds from the dipped plants, they were grown on selective MS-agar plates to find successfully transformed T_1 plants. The resistant ones were then transferred to soil for further growth. From the next generation, T_2, 30 seeds were put on selective MS-agar plates, as shown in Figure 8, to screen them for single insertion, which results in a 1:3 mendelian segregation.

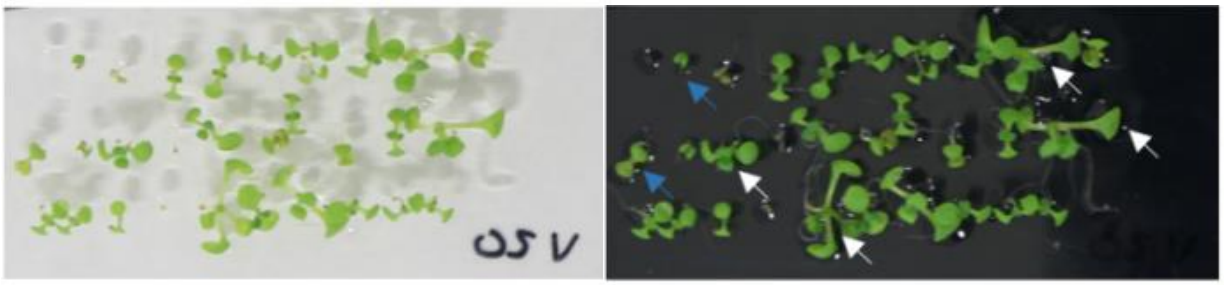

Figure 8: Example for T2 selection
White arrows indicate resistant seedlings and blue arrows indicate hygromycin sensitive seedlings

2.2.6.3 Protein extraction

From lines that showed a segregation of 65-95% resistance, 10 seedlings were collect, treated overnight with 5µM Bortezomib, and frozen in a 2mL-tube with 2 metal beads in liquid nitrogen. To extract the proteins from these plants, they were pulverized in a TissueLyser and 100µL protein extraction buffer were added. After homogenization, the samples were heated for 6 minutes at 95°C and pelleted by centrifugation at 20000xg and RT for 10 minutes. The proteins in the supernatant were then transferred to fresh 1.5mL-tubes containing 30µL sample loading dye and stored at -80°C until analysis by SDS-PAGE and Western blot.

3 Results and Discussion

3.1 Development of the yeast strain CB80ΔUBR1 – KanMX

For functional reconstitution of plant E3 ligases in *S. cerevisiae*, Telser, T. developed a strain lacking its only N-recognin UBR1, CB80ΔUBR1. This strain was used for the experiments with PRT6 of this work. As it could be interesting to inhibit the translation at some point of these experiments, we checked, if the KanMX cassette in this strain, which provides geneticin resistance, affects the influence of CHX treatment on the cells.

Therefore, we did a growth experiment in YPD medium, with the CB80 wild type strain, which should be affected by cycloheximide, as negative control, and the CB80ΔUBR1 strain, to see potential differences. As positive controls, we used both strains without CHX treatment for comparison, to check if they grow equally well. Pre cultures of 50mL were grown over night and used to inoculate the 10mL main cultures for treatment to an OD_{600} of 0.1 to 0.2, always as triplicates for each strain and used CHX concentration, 0, 0.5, 5, 50 and 100µg/mL, which makes 30 flasks in total. Optical density of the main cultures was measured in different dilutions at time points 0, 4, 21, 25, 28.5, and 45 hours after inoculation of triplicate main cultures. The results are shown in Figure 9 below.

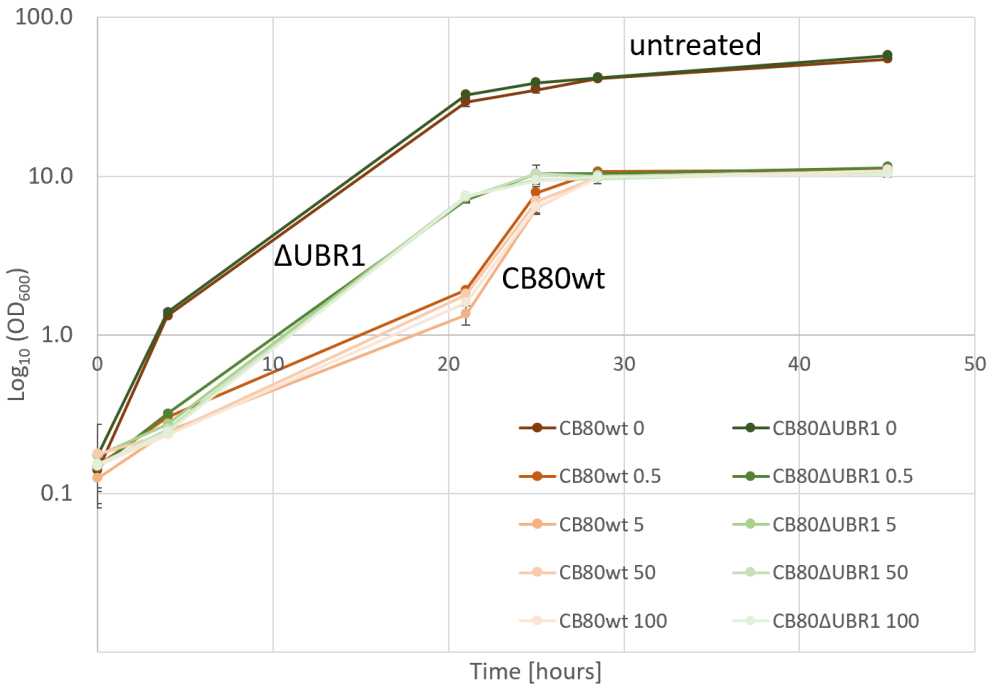

Figure 9: Growth assay with cycloheximide treatment to compare CB80wt (red) and CB80ΔUBR1 (green) CHX concentrations from 0 to 100 µg/mL indicated with darker to lighter colors over 45 hours

The wild type strain is indicated in orange and the UBR1 deletion strain with green lines. Additionally, the lower concentrations are indicated with darker colors and get lighter with increasing CHX treatment. The untreated positive controls show very similar curves, which proves, that the deletion itself does not change the growth of the cells. After around 20 hours, the stationary phase was reached with an optical density of approximately 30. For the treated CB80ΔUBR1 cells, shown in light green lines, the curve looks similar to the untreated ones, but was shifted to slightly lower optical density. Compared to this, one can see a clear delay of growth for the treated wild type cells (light orange lines) away from the deletion strain curves, which starts around 5 hours after inoculation and cures after roughly 23 more hours. On top of this, there seems to be no dosage dependency for cell growth between 0.5 and 100 µg/mL CHX treatment.

Due to this clear difference between the two strains, we concluded that the KanMX cassette makes cells less susceptible to treatment with the translation inhibitor cycloheximide. We planned to remove the KanMX cassette and develop the new CB80ΔUBR1 – KanMX strain, which should show a similar reaction to CHX treatment as the wild type strain.

After developing this new strain according to 2.2.3.4, we repeated the growth experiment as above. The results are depicted in Figure 10. As we saw no dosage effect in the first experiment, we decided to use concentrations of 0, 0.1 and 0.5 µg/mL CHX this time, and to stop the measurements already 21 hours after inoculation of the main cultures.

Like before, wild type growth is indicated with orange lines, CB80ΔUBR1 with green and CB80ΔUBR1 – KanMX with yellow ones. Again, the untreated positive controls, indicated with the darkest colors, show very similar growth for all three strains. Unfortunately, we could not observe any difference in growth for the treated cells, neither between the strains, nor for the various CHX concentrations.

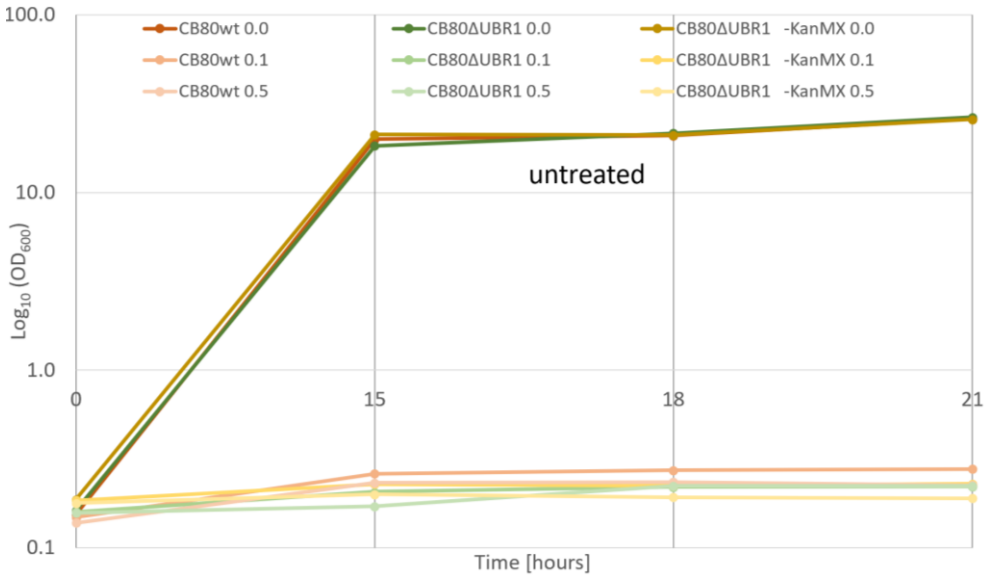

Figure 10: Growth assay with CHX treatment to compare CB80wt (red), ΔUBR1 (green) and ΔUBR1 – KanMX (yellow) with CHX concentrations from 0 (darkest shade) to 0.5µg/mL (lightest shade) over 21 hours

Another approach to make possible differences between theses strains visible, could be to perform a tFT assay with different concentrations of CHX or even with other translation inhibitors. As there was not the time to validate this result, and the strain was anyways developed, we decided to use it for the BIG experiments of this work.

3.2 Validation of tFT reporter constructs

To further validate the tFT reporter constructs described by Böhm et al. 2023, substrates with several different N-termini were tested. To make sure the degradation activity depends on PRT6 (AT5G02310), the substrates were transformed into a yeast strain containing the complete plasmids to express UBC2 and PRT6 (+PRT6; green bars) or to a strain containing the complete plasmid to express UBC2 but only the empty vector of the PRT6 plasmid (-PRT6; grey bars). The results of the experiments were calculated, as explained in the material and methods part of this work, for data collected around 24 hours after inoculation of the 96-well-plate. For the graphic depicted in Figure 11, at least 18 data points were pooled with additional data from experiments performed by Winter N. and normalized to the stable control with N-terminal valine (V), shown on the left side.

For the strains lacking PRT6, the average of the pooled data varies between 80% and 110% of V-tFT, shown in grey bars. Compared to this, the green bars for the strains expressing PRT6, clearly show degradation activity for basic (type I) N-degrons H-, K-, D- and R-tFT.

Surprisingly, also degradation of hydrophobic (type II) N-degrons F-, L- , Y- and W-tFT by around 30% in average could be observed. For the further tested N-termini, ML-, M-, Ile-, A-, and S-tFT, no clear degradation was seen.

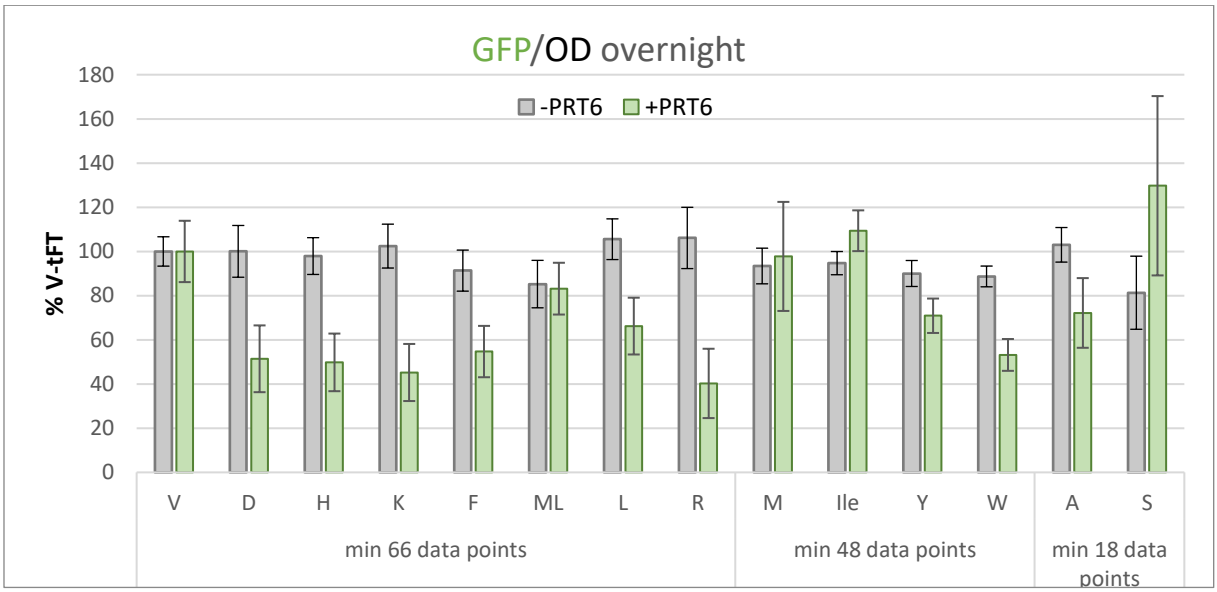

Figure 11: Bar plot for green fluorescence normalized to OD_{600} for different N-degron substrates +PRT6 (green bars) and –PRT6 (grey bars) with values from overnight measurement, referred to V-tFT, set to 100%

These trends could also be confirmed by looking at the ratio of red to green fluorescence for the measurement taken 2 hours after inoculation of the 96-well-plate, depicted in Figure 12, even if the averages for +/- PRT6 for each N-degron substrate show less difference.

Additionally, the standard deviation for the strains containing PRT6 is much higher than for the GFP/OD_{600} values above. Therefore, only the green fluorescence normalized to the optical density at 600 nm, after incubation of the main cultures for 24 hours is shown for the following experiments.

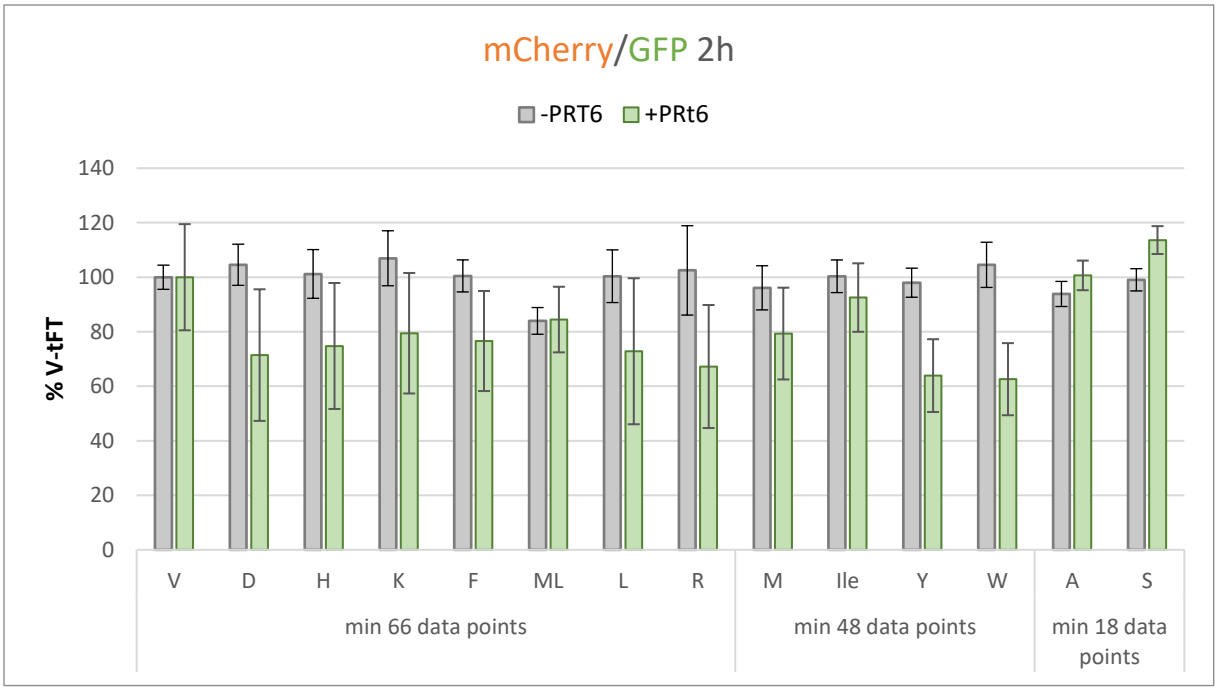

Figure 12: Bar plot for red per green fluorescence for different N-degron substrates +PRT6 (green bars) and -PRT6 (grey bars) with values from measurement 2 hours after treatment, referred to V-tFT, set to 100%

Nevertheless, the tandem fluorescent protein timers are interesting to see possible differences in degradation efficiency for specific N-degrons between 5 and 40 minutes, due to the maturation times of the fluorophores after translation as explained in the introduction. Furthermore, they might be less influenced by factors such as the plasmid copy number per cell or growth conditions and therefore could be more accurate in some cases.

3.3 Mutation of PRT6 UBR box domain

As UBR1 is the only N-recognin in yeast, schematic depiction shown in the upper part of Figure 13, it degrades type I as well as type II N-degrons. Tasaki et al. 2012, Holdsworth et al. 2020 and (Pan et al. 2021) described it with a UBR box domain (green) for degradation of basic N-degron substrates and a ClpS-like motif (white) for substrates with hydrophobic N-termini. A sequence alignment from Schleiffer, A. (IMP), of plant PRT6 to the UBR1/2/3 protein family, showed a separation into proteins that contain both domains, UBR and ClpS, from the UBR 1 and 2 protein families and one that contains proteins with only the UBR domain and lack a ClpS-like motif, which PRT6 and proteins from the UBR3 family belong to. Additionally, he did a search on the *A. thaliana* proteasome for a ClpS-like motif, which only matched with the chloroplastic Clp protease adapter protein CLPS1. Based on these findings, and the sequence homology of yeast UBR1 and plant PRT6, schematic comparison

shown in Figure 13, it is unlikely that PRT6 also has a ClpS-like motif. It remains unclear how PRT6 can recognize hydrophobic N-degrons as demonstrated in the previous part of this work.

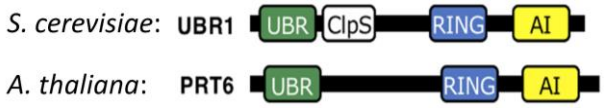

Figure 13: Schematic comparison of S. cerevisiae UBR1 and A. thaliana PRT6 (Holdsworth et al. 2020)

As there is no structure available for PRT6, we decided to interrupt the binding function of the UBR box domain in PRT6 to see if there is another region for interaction with type II substrates. Therefore, we used the UBR box domain sequence alignment shown in Figure 14, the published structure of yeast UBR1 (Pan et al. 2021), and the predicted structure of PRT6 from AlphaFold (EMBL, Hinxton, UK). With all this information and the expertise from Hodakova, Z. and Haselbach, D., we decided to mutate the residues D(140), D(171), D(174) and E(175), indicated with violet boxes, to alanine, to neutralize the negative charge of the binding pocket.

Figure 14: Sequence alignment of A. thaliana PRT6 and S. cerevisiae UBR1 (Kim et al. 2022)
Mutations indicated with violet boxes D(140), D(171), D(174) and E(175) were changed to alanine

The results for this experiment are shown below in Figure 15. The values for degradation of the different N-degron substrates in the yeast strains with the UBR box domain quadruple mutant PRT6 variant shown in violet, range between roughly 90 and 100% V-tFT. This makes a huge difference compared to the set-up with the intact wild type PRT6 shown again in green and leads to the conclusion, that both N-degron types might interact with the UBR box domain.

Additionally, the repetition of the experiment with wild type PRT6 also confirmed the previous finding of interaction with type II N-terminal amino acids and further supports the assumption that the interaction with basic N-degron substrates is preferred compared to hydrophobic ones, as shown by their enhanced degradation.

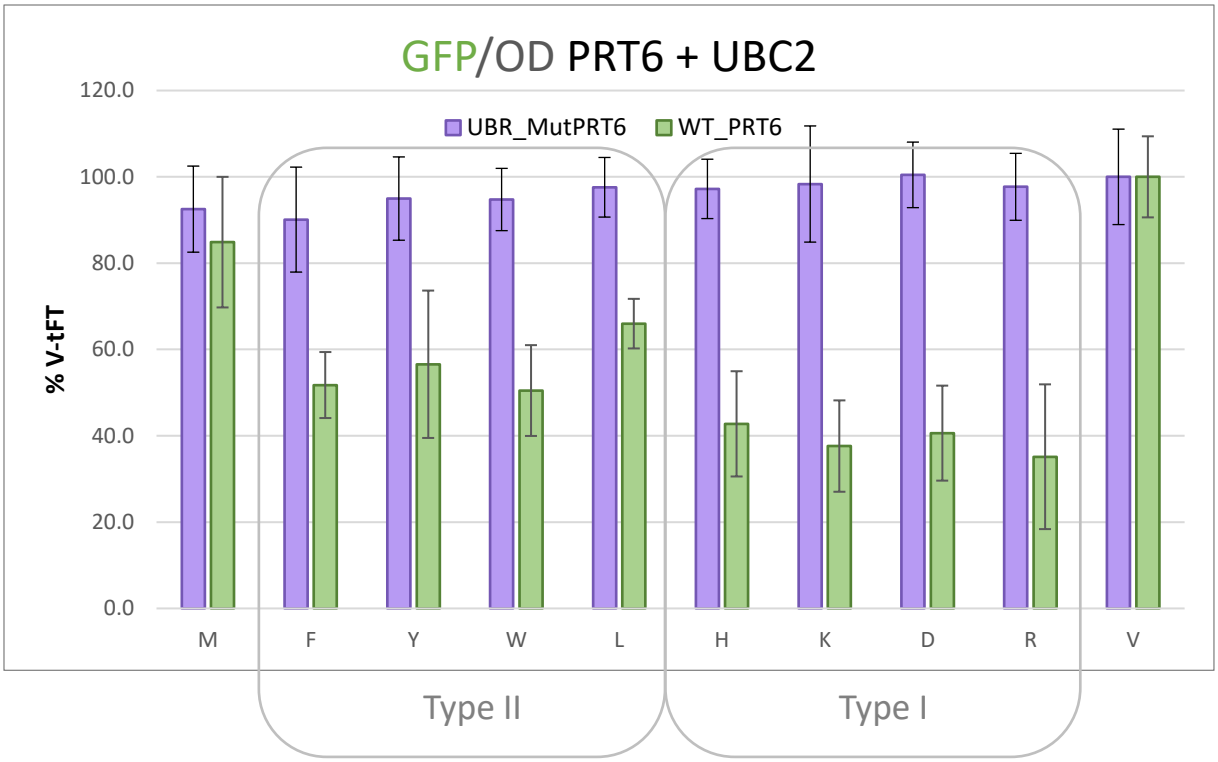

Figure 15: Bar plot for quadruple PRT6 UBR domain knock out mutant, UBR_MutPRT6 (violet) compared to wild type, WT_PRT6 (green) with values from overnight measurement, referred to V-tFT, set to 100%

Because of the complete loss of function, we cannot rule out that the mutations have led to a misfolded and subsequent degraded protein. Unfortunately, we used the untagged version of PRT6 for this experiment and lack an antibody against it, so we could not check with a Western Blot if just the binding function of the UBR box domain was interrupted or if the mutations caused the degradation of the whole protein. Assuming, that the UBR box domain of the protein interacts with both types of N-degrons, we started the next mutagenesis round, where we tried to interfere with the interaction of only one of the two types of N-degrons.

For the following experiments, we used the PRT6 with a 3xHA-tag, to have the opportunity of detecting it on a Western Blot if the protein again loses its function with the next mutations. As the mutation of a single domain as a way to interrupt only binding of one of the two types of N-degrons is really complicated, we decided to ask Hodakova, Z., a structural biologist from the research institute of molecular pathology (IMP) for help. She suggested the hypothesis, that the penultimate residue of hydrophobic N-degrons mediates the binding of the substrates to the UBR domain of PRT6. Therefore, she recommended to start with testing three different double mutants, shown in Figure 16. The mutation of DE

(174, 175) to AF (blue bold letters, second line) should block the binding pocket structurally. The mutation of the same residues to AK (orange bold letters, third line) adds additionally a positive charge, which should selectively interfere with the interaction with positively charged, type I N-degrons. The third mutant contained the change of W and A (125, 144) to A and S (yellow bold letters, last line) and should modify the surface of the UBR domain that interacts with the penultimate residue of hydrophobic N-degrons in a way, to selectively interfere with the recognition of type II N-degrons.

Figure 16: Sequence alignment of A. thaliana PRT6 UBR box domain wild type and double mutants
Mutant AF: DE (174, 175) mutated to AF indicated with blue bold letters
Mutant AK: DE (174, 175) mutated to AK indicated with orange bold letters
Mutant AS: W and A (125, 144) mutated to A and S indicated with yellow bold letters

The results for the first mutant, PRT6_AF, are shown as blue bars in Figure 17. The first important observation is that the mutant is still active. Compared to the wild type version shown in green, there might be a slight reduction in degradation of type I N-degrons, but a clear difference in degradation of type II substrates, except isoleucine.

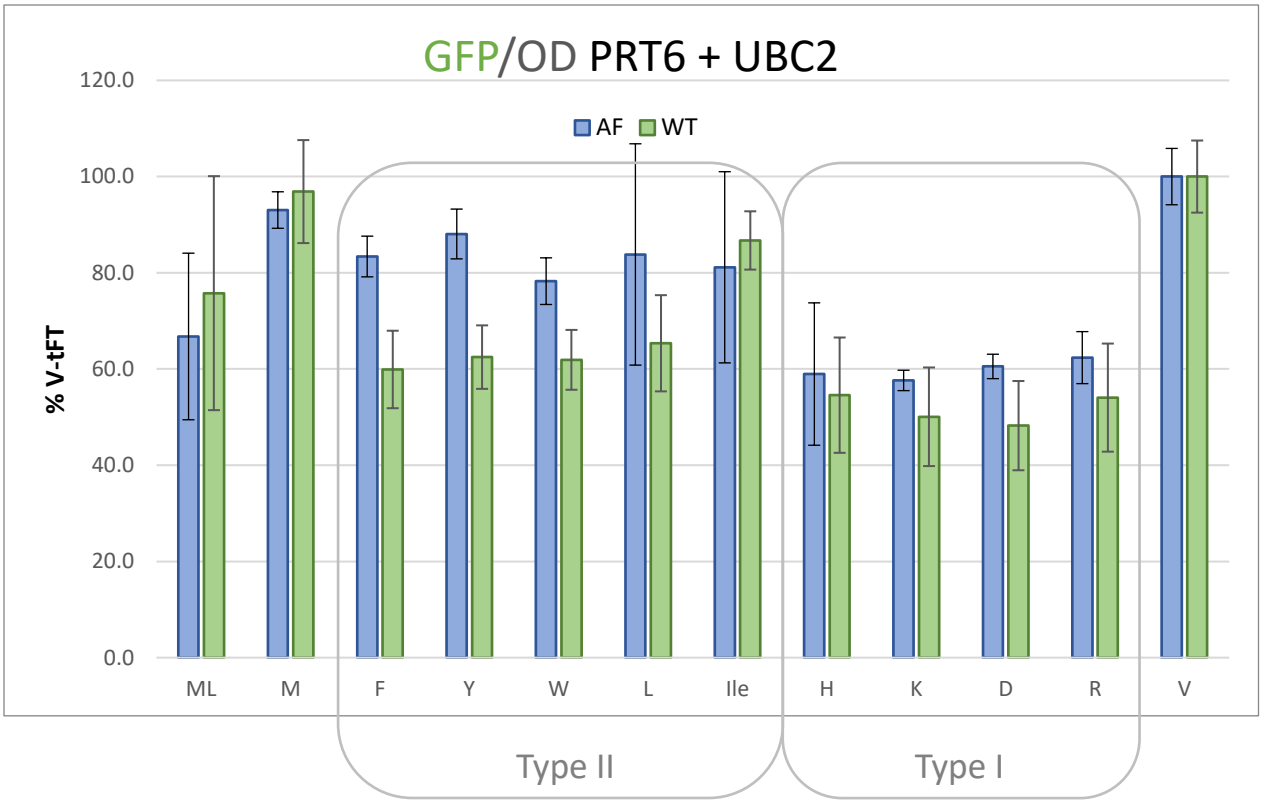

Figure 17: Bar plot for double mutant AF PRT6 (blue) and wild type (WT) PRT6 (green) with values from overnight measurement, relative to V-tFT, set to 100%

The results for PRT6 mutant AK, which has point mutations at the same residues but an additional positive charge from the lysine, is shown in orange bars in Figure 18. Surprisingly, it shows no convincing difference in degradation activity compared to the wild type PRT6 control in green. Only the degradation of the substrate with N-terminal leucine seems affected.

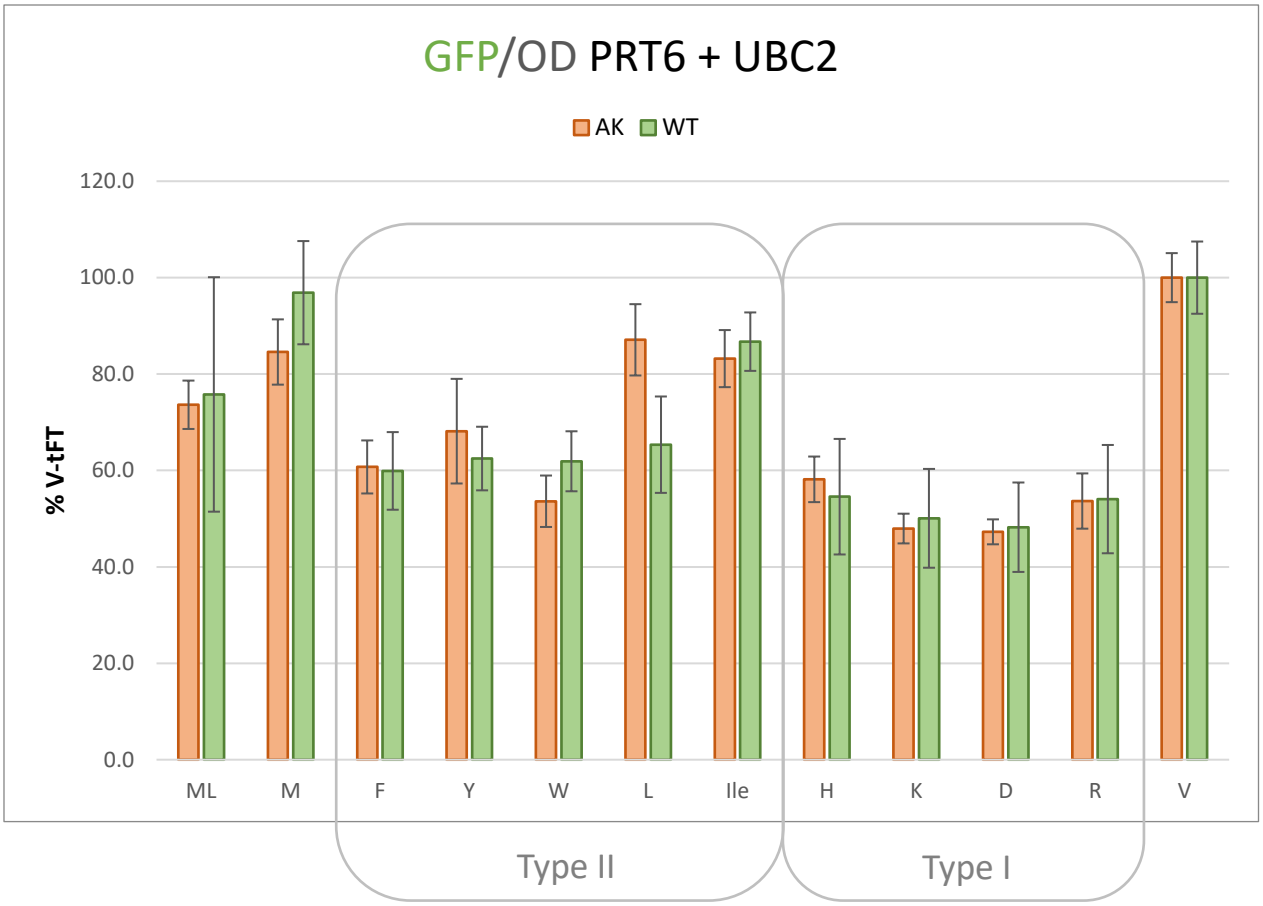

Figure 18: Bar plot for PRT6 double mutant AK (orange) compared to wild type PRT6 (green) with values from overnight measurement, relative to V-tFT, set to 100%

The third mutant should affect the binding of type II N-degrons. Therefore, two residues that are supposed to bind to the backbone structure of the N-terminal end of the substrates were mutated. The results are shown as yellow bars in Figure 19. This mutant acted as expected and reduced the degradation of substrates with hydrophobic N-terminal amino acids.

As there was no complete loss of function for these mutations, no Western Blots were done. Also, the experiments were only done once, because of lack of time. The experiments are repeated in the lab by O. Rudi and show similar degradation patterns.

The next steps will be to test new mutants, designed based on these results. As the mutants AF and AS both seem to affect type II substrate binding, I would suggest testing some kind of combination of these mutations.

Furthermore, it might be interesting to try to find mutations that affect type I but not type II substrate degradation, which could give a deeper insight into the binding mechanism of the UBR box domain.

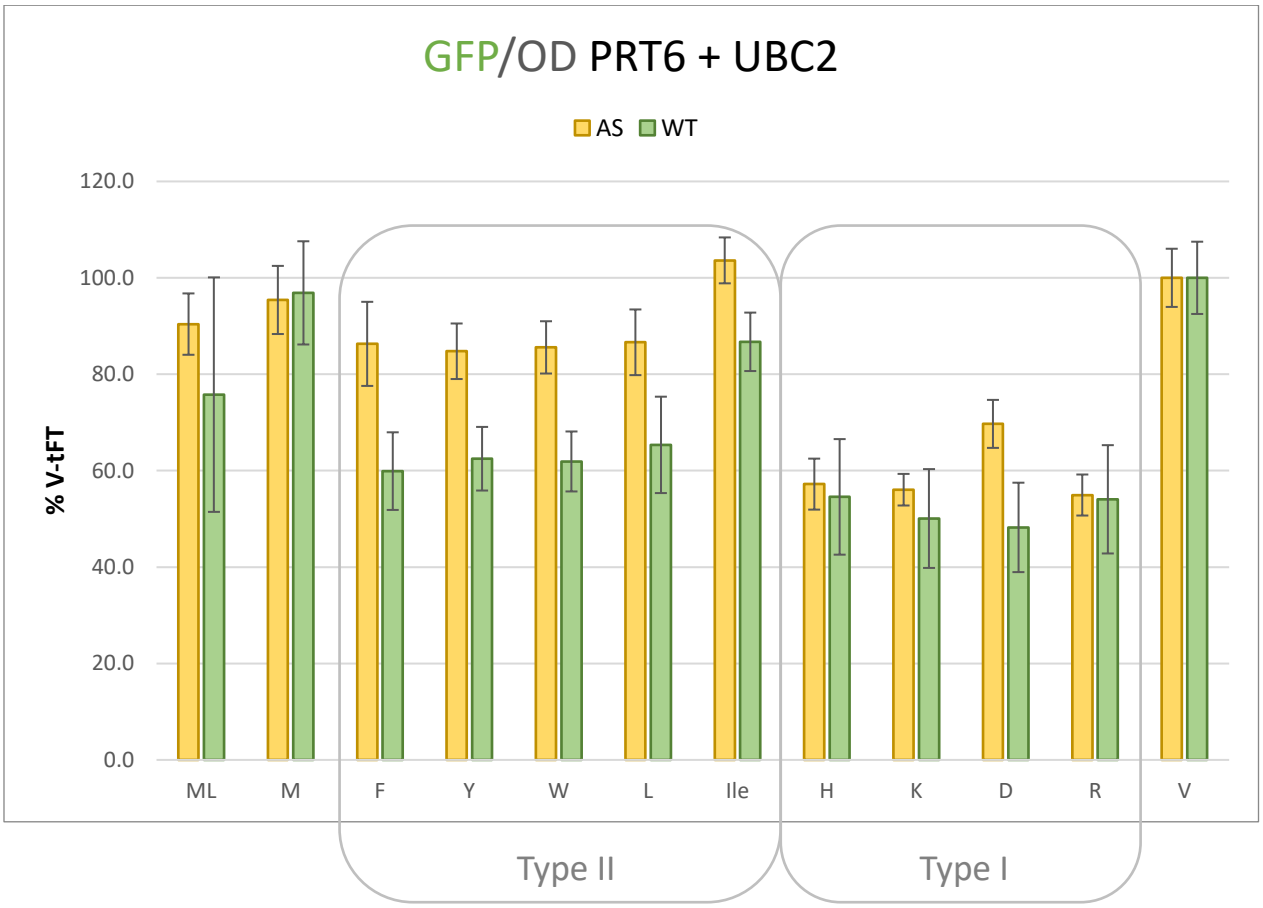

Figure 19: Bar plot for PRT6 double mutant AS (yellow) compared to WT PRT6 (green) with values from overnight measurement, relative to V-tFT, set to 100%

Additionally, Grishkovskaya, I. (IMP) in the lab of Haselbach, D. managed to purify PRT6 from insect cells in order to determine the structure by cryo electron microscopy (EM). When this procedure is successfully established, one could add different ligands in form of oligopeptides to map the precise interaction surface in the UBR box domain.

3.4 Functional reconstitution of potential plant E3 ligase BIG in yeast

The second protein of interest for this work is BIG (AT3G02260). Here, it was not even clear if it acts as E3 ligase or N-recognin. The only hint for this was a slight increase of biotinylation of the protein for the interaction with a substrate with N-terminal arginine compared to methionine, in the Turbo-ID labelling experiments performed by Winter, N. (Zhang et al. 2023), which could have several reasons besides BIG being an N-recognin. To test if BIG acts

as E3 ligase, we first had to establish an environment for the protein to be active in yeast. In a first experiment, we tried the co-expression with UBC2 or the other plant E2 enzyme UBC3 (AT5G62540), where we could not detect any degradation activity towards substrates. The mammalian homologue to BIG is UBR4 (Kim et al. 2018) and known to need a HECT E3 ligase (KCMF1, Hong et al. 2015) for substrate degradation. As UPL2 (AT1G70320) is also preferentally labelled in the Turbo-ID labelling experiment (Zhang et al. 2023), and known to be co-expressed with BIG (Cococo-Net online tool), we decided to add this HECT E3 ligase, cloned by L. Nehlin to the system. The combination of BIG, UPL2 and UBC2 showed degradation activity in the yeast system, shown as green bars in Figure 20. Because the plant turbo ID labelling experiments mentioned before showed that BIG interacts with a substrate with N-terminal arginine, we used this N-degron, as in the previous experiments, as degradation control. To have a first idea if the system also interacts with type II N-degrons, we took the L-tFT substrate as third candidate, and indeed found that it is potentially degraded, although to a smaller degree than R-tFT.

To validate that both E3 ligases are needed in this system, we tested it with an empty BIG vector, shown with grey bars and with an empty UPL2 vector, represented in yellow bars. Additional data for these experiments, for the two different E2 enzymes UBC2 and UBC3, and for GFP/OD_{600} after overnight incubation and red/green fluorescence for 2 hours after inoculation, can be found in the appendix in Figure 32 to Figure 35.

So we established that BIG and UPL2 are both necessary for degradation activity in yeast. Further, we showed that also an E2 enzyme, UBC2 or 3, has to be present for the system to work. Next, we asked whether UPL2 as known HECT E3 ligase (Bates and Vierstra 1999), has just a structural or even a catalytic function. To answer this question, the catalytically active cysteine (C3625) was mutated to an alanine, UPL2mutCA. The results for this last test are shown in Figure 20 in orange bars, and proved that the catalytic activity of UPL2 is essential for the function of this system.

It is worth mentioning that, for these experiments, the cells needed at least one week growth on selective agar-plates and two days growth in selective SD medium with 2% galactose and 0.1% glucose before inoculation of the main cultures in 96-well-plates for measurement.

Unfortunately, there was not enough time to repeat the experiment with mutated UPL2 because the cells were maybe already too old and grew not well enough to detect a proper signal. Simply streaking them newly out on fresh agar plates was not enough to refresh them. One should try to retransform the plasmids into the used CB80ΔUBR1 – KanMX strain.

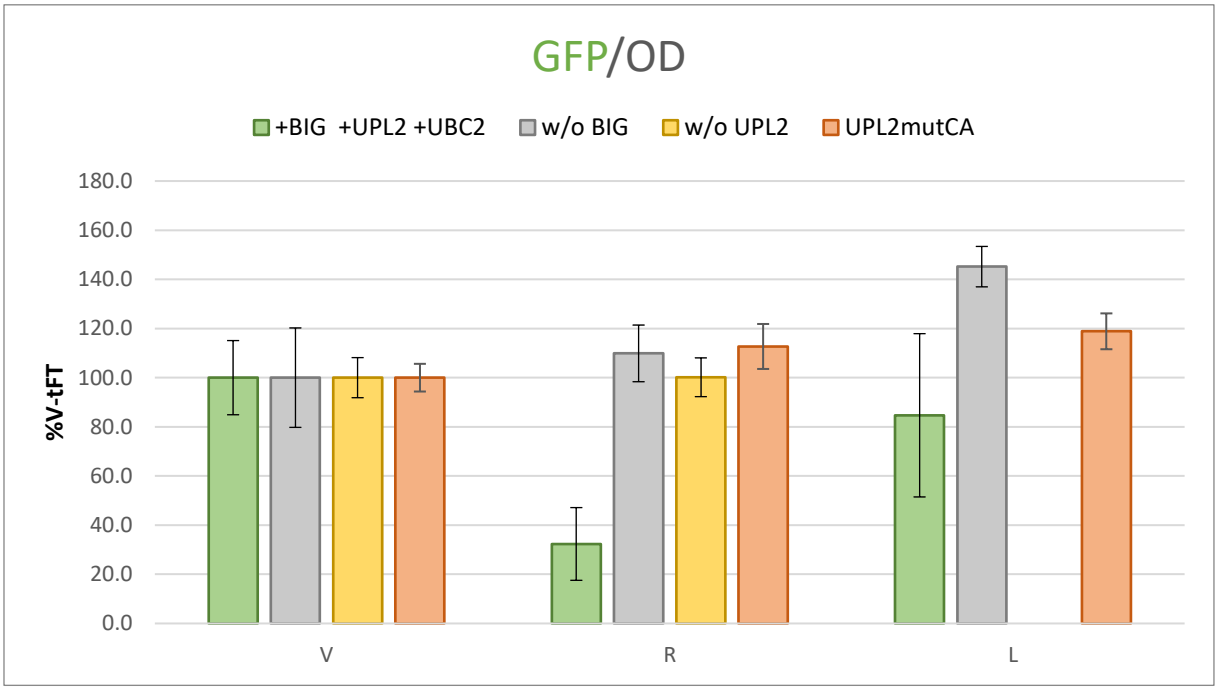

Figure 20: Bar plot for BIG + UPL2 + UBC2 (green), empty BIG vector + UPL2 + UBC2 (w/o BIG, grey), BIG + empty UPL2 vector + UBC2 (w/o UPL2, yellow) and BIG + UPL2 active site C mutated to A + UBC2 (UPL2mutCA, orange) with values from overnight measurement, relative to V-tFT, set to 100%

If the results of these experiments can be reproduced, in a next step the calcium dependency of the system could be tested. Therefore, one should microscopically check if BIG is in yeast, as in plants (Modrego et al. 2023), associated to the ER and important for the maintenance of organelle movement. If this is the case, experiments with calcium channel inhibitors, calcium ion chelators or increased extracellular calcium concentrations could give an idea of the influence of Ca^{2+} on this system. On top of this, monoubiquitylated substrates could be tested in combination with BIG and UBC2, which might identify BIG as chain elongator.

3.5 Testing tFT reporter constructs in plants

Besides the general principle of function, also the localization in specific tissues and subcellular localization in different developmental stages of plants is very interesting. Therefore, Sandbohr, J. cloned a plasmid containing different selection markers and a

tandem fluorescent protein timer reporter construct with N-terminal R and V, shown in the upper part of Figure 21.

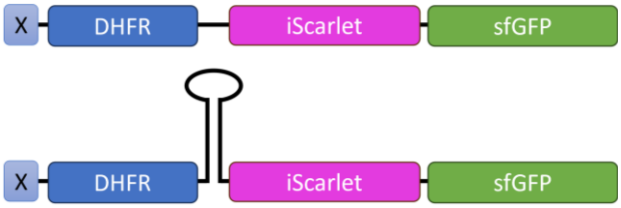

Figure 21: Schematic depiction of old (upper part) and new (lower part) plant tFT reporter constructs, different N-terminal amino acids represented by X

To get a first idea if a reporter is degradable in principle, one can infiltrate *N. benthamiana* leaves with *A. tumefaciens* carrying the vector for transient expression of the protein. Figure 22 shows results from those infiltrations done by J. Sandbohr, recorded after 48 hours, for constructs with N-terminal arginine (unstable) and valine (stable). On the left side of the image, the green fluorescence signal from the leaves is shown and on the right side the red one. One can clearly see that the first reporters, shown on the right side of the bigger depicted leaves, did not show the expected results, as R-tFT seems even more stable than the normal used stable control V-tFT, in the green as well as in the red channel. Therefore, the Bachmair Lab decided to introduce a loop for potentially better proteasomal entry to the new version of the constructs, schematic depiction shown in the lower part of Figure 21. For the new version, R-tFT has a lower fluorescence signal in both channels compared to V-tFT for the infiltrations done by J. Sandbohr, which indicates increased degradation.

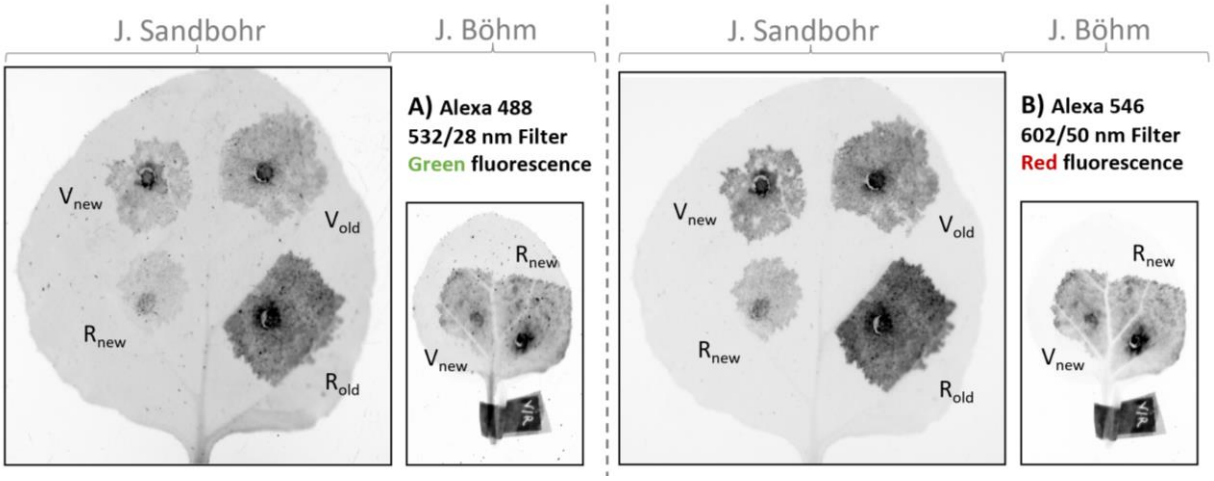

Figure 22: N. benthamiana infiltration example for V- and R-tFT reporter constructs, 48hours after infiltration, with additional results from J. Sandbohr for an older and the new version shown in bigger squares, left side for green fluorescence, right side for red fluorescence

Before floral dipping of *A. thaliana*, the infiltration experiment with the new reporter constructs was repeated. Results for these, done by myself, are shown with the smaller depicted leaves. Unfortunately, this time both constructs seem to have the same fluorescence intensity in both channels and therefore no difference in degradation. Infiltrations were done with all newly cloned N-terminal amino acid constructs, always with V-tFT on the left side of the leaf and the tested N-degron on the right side. Results for these further infiltrations are shown in the appendix in Figure 36, all for 48 hours after infiltration. Additionally, we had a look at the constructs over time, which also did not show any degradation differences. These results can be found in Figure 37 to Figure 40 of the appendix.

Nevertheless, we decided to transform *A. thaliana* plants with these constructs as there may be many reasons why the repetition of this experiment done by another person could have failed.

3.6 Identification of potential plant lines for microscopy

To identify successfully transformed *A. thaliana* plants, the first generation was screened depending on the hygromycin selection marker on MS+Hyg+Vanco+Cefo-agar plates. Resistant plants of this generation were transferred to soil for further cultivation. The next generation was then screened for single insertions to the genome, which causes a Mendelian segregation pattern. Therefore, 30 seeds of every single plant were put on MS+Hyg-agar plates for selection, where ¾ should show resistance and ¼ should be sensitive according to the Mendelian rule of segregation. Seedlings showing a pattern of 60 to 90% resistance, were collected and frozen at -70°C in tubes containing two metal beads. Proteins were extracted as described in the material and methods part of this work. Figure 23 shows an example for a Ponceau stained Western Blot membrane, to see if the protein transfer from gel to membrane worked in general.

Images of Ponceau stained Western Blot membranes for the further identified Mendelian segregated plant lines are shown in Figure 41 to Figure 47 of the appendix. All of them prove, that the proteins were properly transferred from the SDS-gels to the membranes.

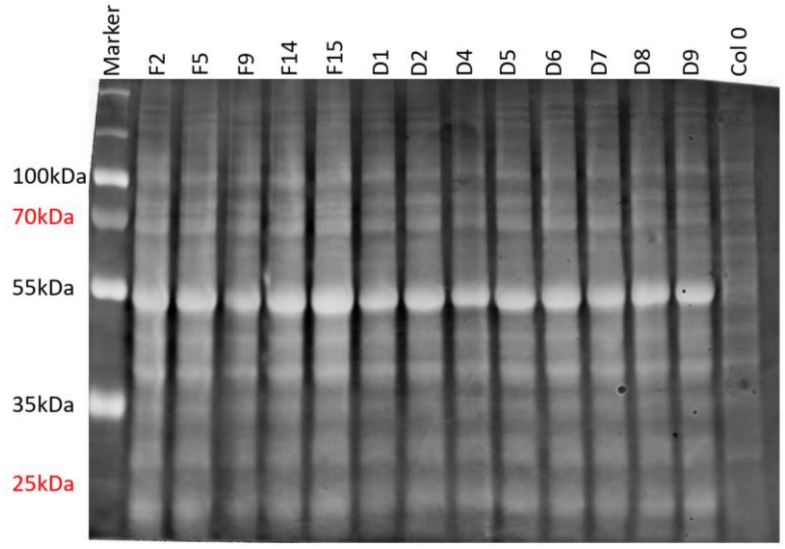

Figure 23: Example for Ponceau stain of Western Blot membrane with plant protein extracts

The next step was then to make sure that the tFT reporter constructs are expressed. For this, a primary antibody from mouse against GFP and a secondary HRP-antibody against mouse IgG were used. For detection, a HRP-substrate solution was added and images were taken with the chemiluminescent settings of a ChemiDoc, as described in chapter 2.2.1.8 of this work. An example for this labelling is shown in Figure 24, with Col0 as negative control on the right, to exclude any signals from unspecific binding events. The highest band between 70 and 100kDa indicates the tFT reporter constructs with a size of 83.3kDa. The lower bands show a degradation product from the whole protein and GFP on its own with 27kDa.

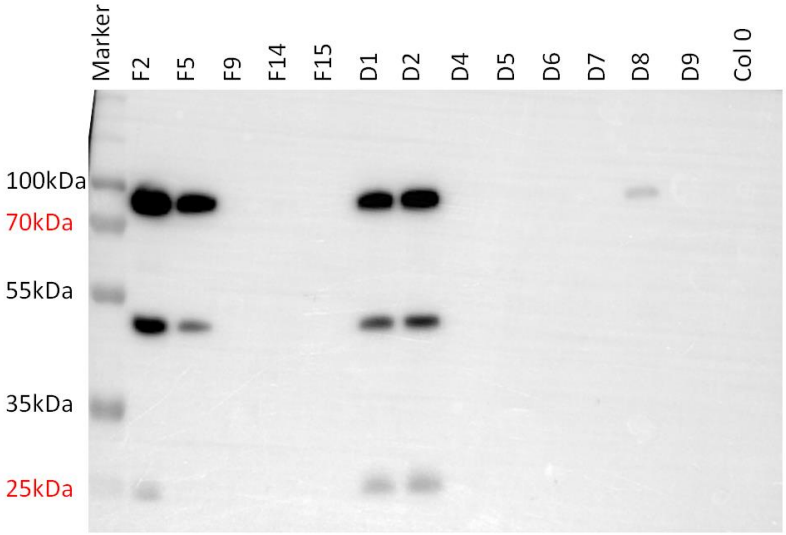

Figure 24: Example for Western Blot membrane with antibody labelled tFT reporter constructs, Col0 as negative control on the right side

Antibody labelled images for the further Western Blots are also shown in Figure 41 to Figure 47 of the appendix. With this method, one can not only identify lines that express the reporter construct, but also to which level. Luckily, we found lines for every N-degron expressing the protein in roughly the same intensity.

For the next generation, one can choose plant lines expressing the protein in higher or lower levels, to check what might be better for microscopy.

With these lines, the stability of different N-degron substrates can be analyzed and might confirm the findings from the transient expression experiments of J. Sandbohr. Additionally, the subcellular localization of the reporter can be detected in the confocal microscope, to determine whether degradation takes place in the cytoplasm by proteasomes, or in the vacuole. To increase these effects, one can use inhibitors for different parts of the N-degron pathway. On top of this, it might be possible to identify tissue specific degradation levels for reporters with different N-terminal amino acids, which may additionally depend on the developmental stage of the plants. Furthermore, one could transform them into mutant plant lines to visualize potential differences.

4 Conclusion and Outlook

Aim of this work was on the one hand the further investigation on PRT6 substrates and interaction sites. Here, we found that PRT6 can interact with basic and hydrophobic N-degrons through the same domain. Furthermore, we started to test some mutations of the PRT6 UBR domain to interfere with the degradation of one of the two substrate types, and indeed identified mutations that influence recognition of type II substrate. These mutations are now candidates for further combinations for complete interruption of degradation of hydrophobic substrates.

On the other hand, this work directly contributed to the discovery of BIG in combination with UPL2 and UBC2 as N-recognin. It was also shown that the HECT domain of UPL2 has a catalytic function in this system, as degradation was completely stopped by mutating C3625 to alanine. The next step could now be to test if monoubiquitylated substrates can be marked for degradation by BIG and UBC2 alone, which would indicate that BIG acts as chain elongator and UPL2 might add the initial ubiquitin to the substrates. Also, the influence of calcium ions on the system could be analyzed, as the tomato ortholog of BIG, RO, was shown to be sensitive to cytoplasmic Ca^{2+} concentrations (Modrego et al. 2023).

To increase the range of possible yeast experiments, a UBR1 deficient yeast strain lacking the KanMX cassette for Geneticin resistance, CB80ΔUBR – KanMX, was developed. This strain should be sensitive to translation inhibition and could increase the detectable difference between stable and unstable N-degron substrates.

On top of this, foundations for microscopically approaches were laid by transforming different tFT constructs to Arabidopsis thaliana and identification of lines with single insertions expressing the N-degron substrates. With these plants, the subcellular localization of the reporters shall be determined with a confocal microscope. This might indicate whether the substrates are degraded in the cytosol by the proteasome, or in the vacuole. Also, different developmental stages could be investigated to see potential differences in degradation preferences and patterns. Additionally, with the N-terminal cysteine reporter construct the influence of oxygen on degradation of the substrate could be tested.

5 Appendix

5.1 Used Oligonucleotides

Table 30: Sequences of used oligonucleotides

Primer	5’ -> 3’ sequence
AtUBC1 896-	GAG GGA TTT CAA GAG GTT GCA GCA
1106-YADHtup	CCG ACA ACC TTG ATT GGA GAC TT
1599-DHFRq1up	CCG ACT ATC CAA ACC ATG TCT ACT
1734-ubr1up4	CCT ATC ACG GAG CTG AAG AAG TCT
1736-ubr1up6	GTC TCC AAT GAC ACG TTC ACT TGT CT
1848-ubi10pdn1	AGG GTT TCA TAG ATA TCA TCC GAT TT
1965-SCE1K19Rfwd	GAG AGG AGA TCG TGG AGG AGG AAT CAT CCT CAT GGT TTT
2016-c19startdn1	AGT TGA TTC GCC AGG TTC GTC GTT
2369-BIGc3101dn	CAG AAT TGC TGA GAA TGC TTT CAT C
2372-BIGc7984up	ACT GAA TCT CAT TGG TGT CTG CAC
2373-BIGc11815dn	TTA CTC GCT GCC CAA AGC TCA CCT
2374-BIGc12427up	TCA AGA TCA GCA TAT ACA CAG CCT
2415-BIG5094dn	CGA AGA GCT CGG GAT AGA GGA CC
2416-BIG6093dn	ACA AAG GGT GGC TGG ATT GCA TC
2417-BIG7796dn	GCT GCT CCA CCG TCC CTA TAC T
2419-BIG9785dn	TTG TGG ATC GGT GCC TGA ACC CT
2420-BIG10735dn	CGC AAA ATC GCA CTT TTG GGC GTA CT
2422-BIG13930dn	CTT GGA ATG CGT CAA GAG CTA TCT TC
2425-BIG3534up	CTG ATG AAG TAC ACT AGT ATC TAC CC
2456-BIGcDNAPshup2	ATA TCA ATG TGA CCA GTG TCA AGC TTT TTA C
2494-PGKpdn2	TCT CTC TTT CAA ACA GAA TTG TCC
2495-PGKpdn3	GTT TTT CAA GTT CTT AGA TGC TTT CT
2579-PRT6cYCpdn	CCA AAA GAT CCC ATA CCA TGG AGA CCA ACT CTT CTC T
2605-PRT6_519-495up	CCC ACA ATC ACA ACA ACC ACC ACC T
2672-3HA-PRT6dn	AGA TCC CAT ACC ATG TCC TAC CCA TAC GAT GTT CCT
2987-BIGc1570dn	GAG GGT AGT CGT TCT CTC TGT TCC AT
2988-BIGc5896up	CGC CTG CAT TGC CGC CCC AAG AT
2989-BIGc6747up	CCA GCA CCT CAT GCC CTC ATC CAT
2990-BIGc10147up	TCC GAG ACA GGG CGA TTG TTG TAA TAC
2991-BIGc11578up	GAT ATG ATG CCC CTT TCT CCC ATT CC
2992-BIGc14058up	GCC TTC TCT ACA CAC CAT GCA AGC C
3014-CEN-ARSup2	AGC CTC GGC ATT TTG GCC GCT CCT
3024-DHFR Bsaup	GGC CAG GGT AGG TCT CCG TTC TTG C
3091-UbrdelKanMXbridge	CCC CGG GTT AAT TAA GGC GCG CCA GTA GAT TCA AGC CCT CTA CTA TGT TT
3102-UPL2c1-26dn	ATG AAG CTT CGA AGG AGA AGA GCT TC
3104-UPL2c3566-3541	GAA GCT GGC TGT ACA AGA AGC TGC GT
3105-UPL2c3443-3470	GGT CTC ACA GTA AGT GGC TGG TAG ATA C
3106-UPL2c6727-6703	AAC CAT TTC CAC CAC CAG ATC GCC C
3107-UPL2c6666-6691	GGA AGC TCT TGA TGG GCT GGA TCA CT
3121-UPL2c1761-1784	CAT TCC GCA GTG TCT GGA TGC TCT
3125-UPL2c4770-4793	CCA GTT TCT GGA AAA TGG AGG CTT
3130-UPL2c8578-8600	CCT TTA GTG TTC CGT CGG GTG CT
3132-UPL2c10182-10203	GGC GTT GTT TGA TGG GCA GCT T
3203-UPL2c2355-2331	AGC TGA ATG CTG AGG GGA GAA GTT C
3205-UPL2c5269-5245	ACC CAG GAA AAC TCA AGA CAA TGT C
3206-UPLc1868-1895	TAT CTG AAG GCT CTT ACT AGT GAT ACA C

3212-UPLc3782-3754	TGA GTA GCA CCA CTT CGA TTT TCC CTA GT
3232-UbrdelkanMXbridge2	AAA CAT AGT AGA GGG CTT GAA TCT ACT GGC GCG CCT TAA TTA ACC CGG GG
3295-G5tFTXhodn	CTT TGC CGG TAA GCA GCT CGA GGA CGG TAG AAC
3296-G5tFTBsaup	GGC CAG GGT CGG TCT CCG TTC TTG CCA ATC
3297-G5tFTAspup	AGA TCT ATC ACC ACC TCT AAG TCT TAA GAC
3298-G5tFTAspdn	CTT AGA GGT GGT GAT AGA TCT GGT GGT GGT GGC
3299-UPL2c8694-8667	GGC TTG ACA ACT GGG ATA GAA GTG AC
3303-BIG13879dn	GAT GAA ATG AGG CGC CGT GCA TT
3304-PGKtermup4	GCA ACA CCT GGC AAT TCC TTA CCT T
3325-BIGc4475dn	CAA CAG GTC CTT TGG TCC CAA AAC
3326-BIGc4542up	GTG ATA TTG AGC TTC CTT CCT GAT CC
3327-UPL2c1258-1236	GCA CAG CAG TAC TGA CCA AAT GC
3328-UPL2c1177-1199	GAA GCT GGT CTT ATT CCG ACC CT
3329-UPL2c2379-2356	GAG CAC AAT ATT CGG GCA AGA CC
3330-UPL2c2265-2291	GCT ATT CTC TTT ACC TCT TAT GCC TC
3331-UPL2c3623-3601	CGC ACA AAA GTC TCA GGT TCC CT
3350-UBRmut1up	GCA CAA GTT GGA GCA TTC TCG CAT
3351-UBRmut1dn	GCG AGA ATG CTC CAA CTT GTG CAA TC
3352-UBRmut2up	GCT GTT GCA GCC CCA CAA GCA CAA CAA CCA CCA CCT GT
3353-UBRmut2dn	GCT TGT GGG GCT GCA ACA GCA TGG AAA CCT GAT GGT
3354-PRT6Ageup	TTA GCA GAG AAA GTA ACC GGT GC
3379-PRT6_AKup	CCA TCA GGT TTC CAT GCT GTT TTA GCC CCA CAA TCA CAA CAA CC
3380-PRT_DEdn	ACA GCA TGG AAA CCT GAT GGT
3381-PRT6_AFup	CCA TCA GGT TTC CAT GCT GTG AAA GCC CCA CAA TCA CAA CAA CC
3382-PRT6_WAASup	CAT GTC CTA CAC CTA TAT GCT ATA TCA TTC TGT CCA GCG ACA GAG CCA CAA ACA CCT C
3383-PRT6_WAASdn	TAT AGG TGT AGG ACA TGC GAG AAT GAC CCA ACT TGT TCT ATC TGC GTG CCT TGT TTC C
3409-UPL2Kfldn	ACC AGC TAC ACG GTA GGG TCC
3410-UPL2CysAlaup	AGC TGT ATG AGC TGA TGG CAG CCG CT
3411-UPL2CysAladn	CTG CCA TCA GCT CAT ACA GCT TTT AAC CAA C
3412-UPL2Bsiup	ACC TCT GGC GAA GAA CGT ACG T

5.2 Vectors and inserts for cloning

Table 31: Vector restriction digests for cloning backbones

Backbone #	Vector (AB marker)	Restriction enzyme (supplier) and buffer
1	3254_R-tFT 5thGen (Kan)	BsaI (NEB)/XhoI (NEB) r3.1 (10x) buffer
2	3254_R-tFT 5thGen (Kan)	BsaI (NEB)/XhoI (NEB) r3.1 (10x) buffer
3	3254_R-tFT 5thGen (Kan)	BsaI (NEB)/XhoI (NEB) r3.1 (10x) buffer
4	3254_R-tFT 5thGen (Kan)	BsaI (NEB)/XhoI (NEB) r3.1 (10x) buffer
5	3254_R-tFT 5thGen (Kan)	BsaI (NEB)/XhoI (NEB) r3.1 (10x) buffer

6	2631_YCplac22-PRT6 (Amp)	AgeI (NEB)/NcoI (NEB) r1.1 (10x) buffer
7	2631_YCplac22-PRT6 (Amp)	AgeI (NEB)/NcoI (NEB) r1.1 (10x) buffer
8	2631_YCplac22-PRT6 (Amp)	AgeI (NEB)/NcoI (NEB) r1.1 (10x) buffer
9	2631_YCplac22-PRT6 (Amp)	AgeI (NEB)/NcoI (NEB) r1.1 (10x) buffer
10	3411_pADH1UPL2_pGADT7LEU (Amp)	BsiWI (NEB) /KflI (ThermoScientific) KflI (10x) fast digest buffer

Table 32: PCR amplification for cloning inserts

Insert #	Template for PCR insert	Primer pair	T_M
1	2851_pBibHyg_M-Scarlet-sfGFP	3295-G5tFTXhodn 3296-G5tFTBsaup	78°C 80°C
2	2852_pBibHyg_L-Scarlet-sfGFP	3295-G5tFTXhodn 3296-G5tFTBsaup	78°C 80°C
3	2848_pBibHyg_F-Scarlet-sfGFP	3295-G5tFTXhodn 3296-G5tFTBsaup	78°C 80°C
4	2854_pBibHyg_C-Scarlet-sfGFP	3295-G5tFTXhodn 3296-G5tFTBsaup	78°C 80°C
5A	2851_pBibHyg_M-Scarlet-sfGFP	3295-G5tFTXhodn 3297-G5tFTAspup	78°C 66°C
5B	2851_pBibHyg_M-Scarlet-sfGFP	3298-G5tFTAspdn 3296-G5tFTBsaup	76°C 80°C
6A	2631_YCplac22-PRT6	2579-PRT6cYCpdn 3350-UBRmut1up	72°C 70°C
6B	2631_YCplac22-PRT6	3351-UBRmut1dn 3352-UBRmut2up	71°C 83°C
6C	2631_YCplac22-PRT6	3353-UBRmut2dn 3354-PRT6Ageup	81°C 67°C
7A	2779_HA-PRT6_YCPlac22	2672-3HA-PRT6dn 3381-PRT6_AFup	67°C 80°C
7B	2779_HA-PRT6_YCPlac22	3380-PRT_DEdn 3354-PRT6Ageup	67°C 67°C
8A	2779_HA-PRT6_YCPlac22	2672-3HA-PRT6dn 3379-PRT6_AKup	67°C 78°C
8B	2779_HA-PRT6_YCPlac22	3380-PRT_DEdn 3354-PRT6Ageup	67°C 67°C
9A	2779_HA-PRT6_YCPlac22	2672-3HA-PRT6dn 3382-PRT6_WAASup	67°C 79°C
9B	2779_HA-PRT6_YCPlac22	3383-PRT6_WAASdn 3354-PRT6Ageup	80°C 67°C
10A	3411_pADH1-UPL2_pGADT7LEU	3409-UPL2Kfldn	71°C

		3410-UPL2CysAlaup	77°C
10B	3411_pADH1-UPL2_pGADT7LEU	3411-UPL2CysAladn	71°C
		3412-UPL2Bsiup	71°C

5.3 Calculation examples

5.3.1 Fluorescence assay

For the exemplary tFT fluorescence assay calculations, data from the overnight measurement from experiment 25 for N-terms F, Y, W, and L with the PRT6 mutant AF was used. Well G2 was chosen as well x.

$$OD_{600}(well\ x) = 0.825$$

$$OD_{600}(medium\ 1) = 0.042$$

$$OD_{600}(medium\ 2) = 0.038$$

$$OD_{600}(medium\ 3) = 0.040$$

$$OD_{600}(medium\ 4) = 0.039$$

$$actual\ OD_{600}(well\ x) = 0.825 - Average(0.042; 0.038; 0.040; 0.039)$$
$$= 0.825 - 0.040$$
$$= 0.785$$

$$fluores._{green}\ (well\ x) = 30539$$

$$fluores._{green}\ (ß - Gal\ 1) = 200$$

$$fluores._{green}\ (ß - Gal\ 2) = 197$$

$$fluores._{green}\ (ß - Gal\ 3) = 200$$

$$fluores._{green}\ (ß - Gal\ 4) = 206$$

$$actual\ fluores._{green}\ (well\ x) = 30539 - Average(200; 197; 200; 206)$$
$$= 30539 - 201$$
$$= 30338$$

$$fluores._{red}\,(well\ x) = 22970$$

$$fluores._{red}\,(ß - Gal\ 1) = 843$$

$$fluores._{red}\,(ß - Gal\ 2) = 819$$

$$fluores._{red}\,(ß - Gal\ 3) = 1041$$

$$fluores._{red}\,(ß - Gal\ 4) = 1039$$

$$actual\ fluores._{red}\ (well\ x) = 22970 - Average(843; 819; 1041; 1039)$$
$$= 22970 - 936$$
$$= 22034$$

$$Normalized\ \frac{GFP}{OD_{600}}\ (well\ x) = \frac{30338}{0.785} = 38635$$

$$Normalized\ \frac{mCherry}{GFP}\ (well\ x) = \frac{22034}{30338} = 0.726$$

$$\%\ Normalized\ \frac{GFP}{OD_{600}}\ (well\ x) = \frac{38635 \times 100}{49125} = \mathbf{78,6}\%$$

$$\%\ Normalized\ \frac{mCherry}{GFP}\ (well\ x) = \frac{0.726 \times 100}{0.911} = \mathbf{79,7}\%$$

5.4 Additional graphics

5.4.1 Phylogenetic trees

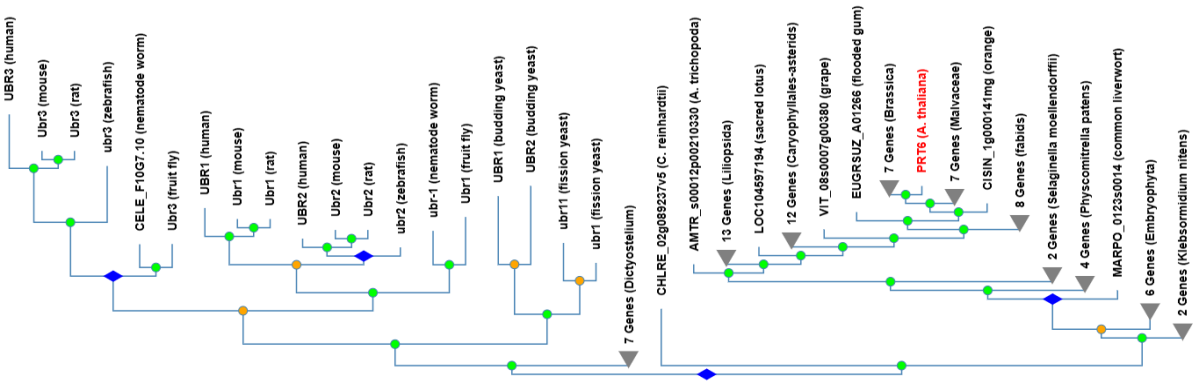

Figure 25: Phylogenetic tree for PRT6 (PhyloGenes (arabidopsis.org)), legend see Figure 26

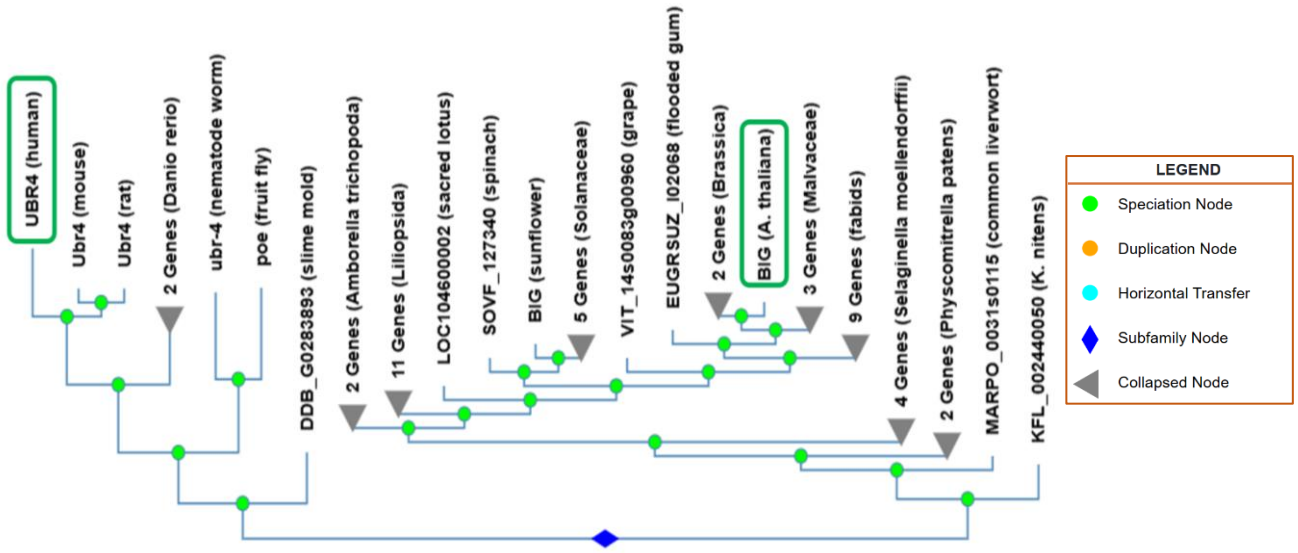

Figure 26: Phylogenetic tree for BIG and UBR4 (PhyloGenes (arabidopsis.org))

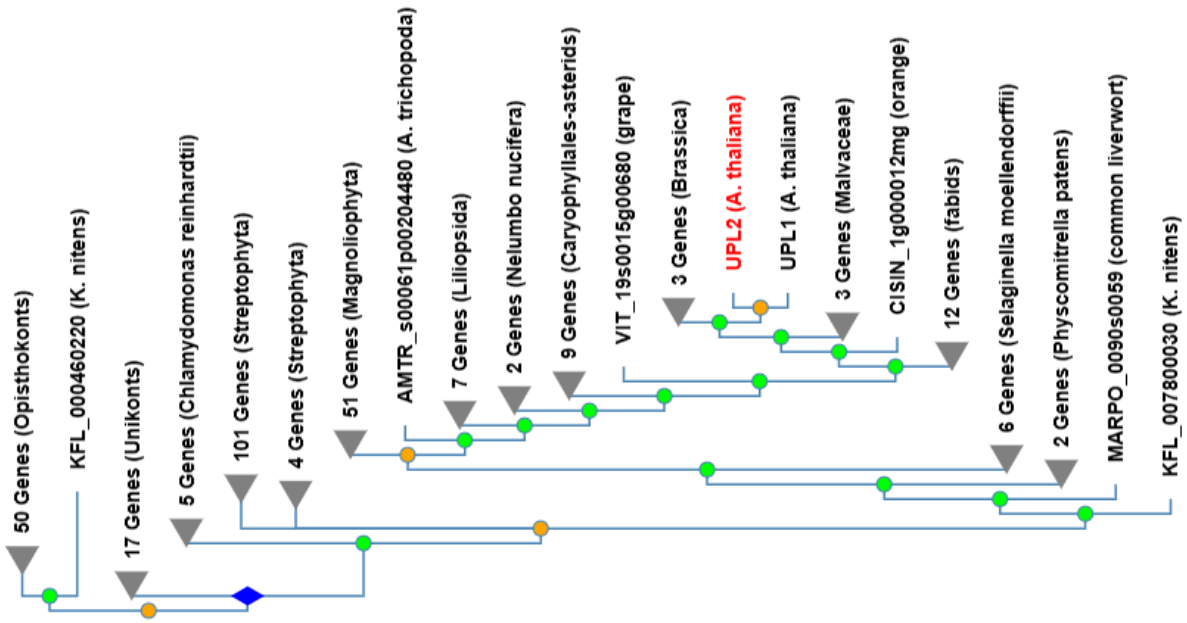

Figure 27: Phylogenetic tree for UPL2 (PhyloGenes (arabidopsis.org)), legend see Figure 26

5.4.2 PRT6

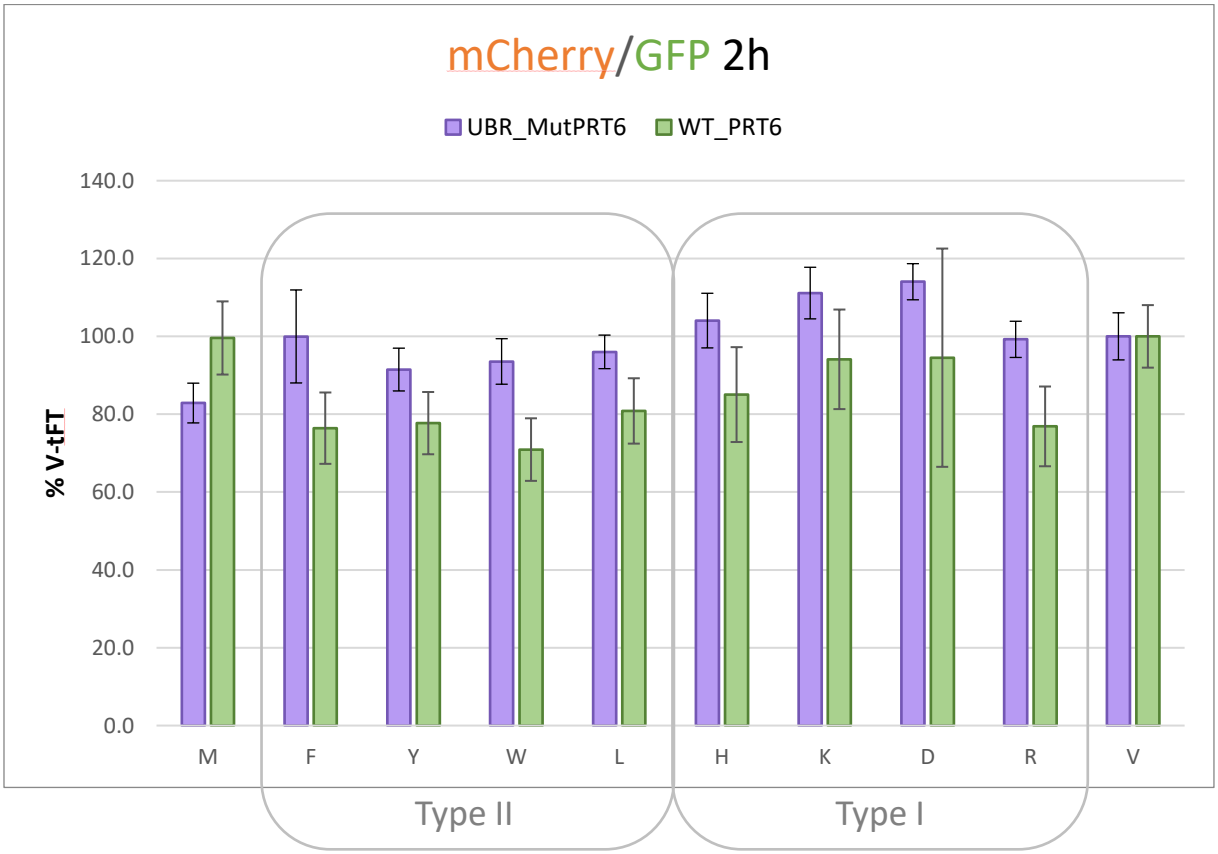

Figure 28: Bar plot for PRT6 quadruple mutant (violet) compared to wild type (green), results for red/green fluorescence after 2 hours incubation, relative to V-tFT, set to 100%

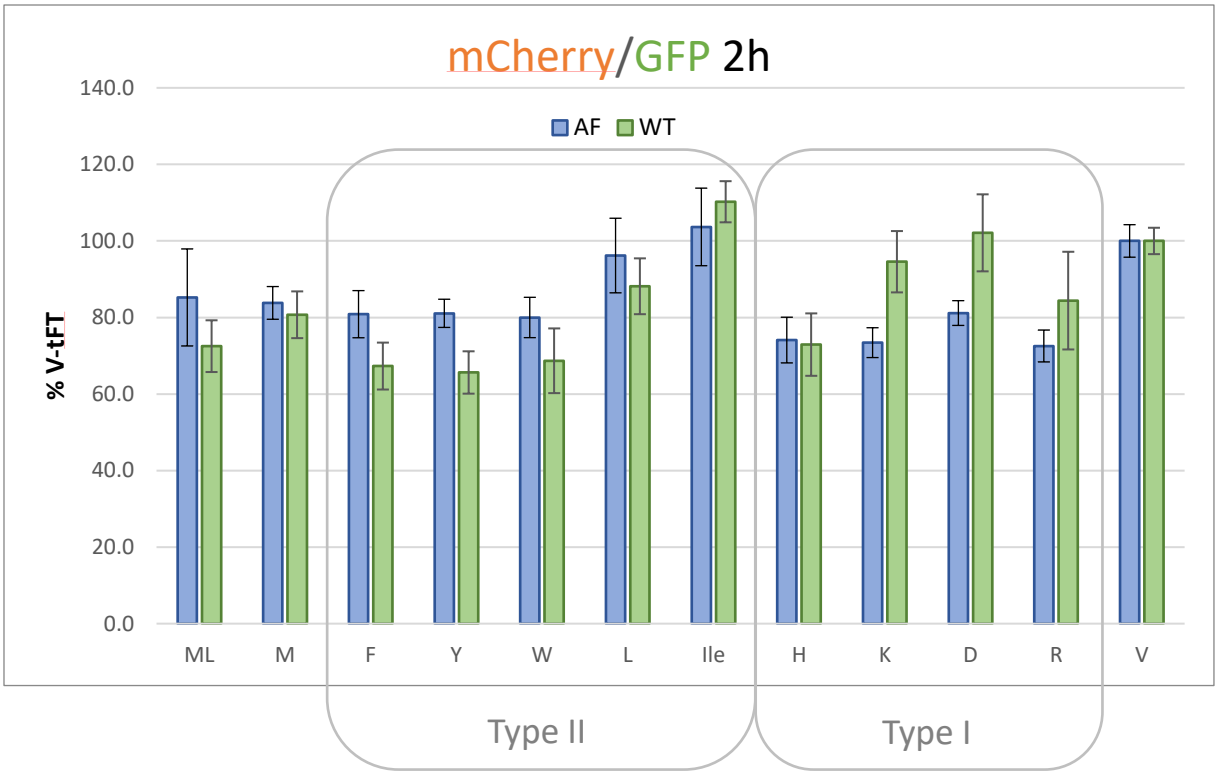

Figure 29: Bar plot for PRT6 double mutant AF (blue) compared to wild type (green), results for red/green fluorescence after 2 hours incubation, relative to V-tFT, set to 100%

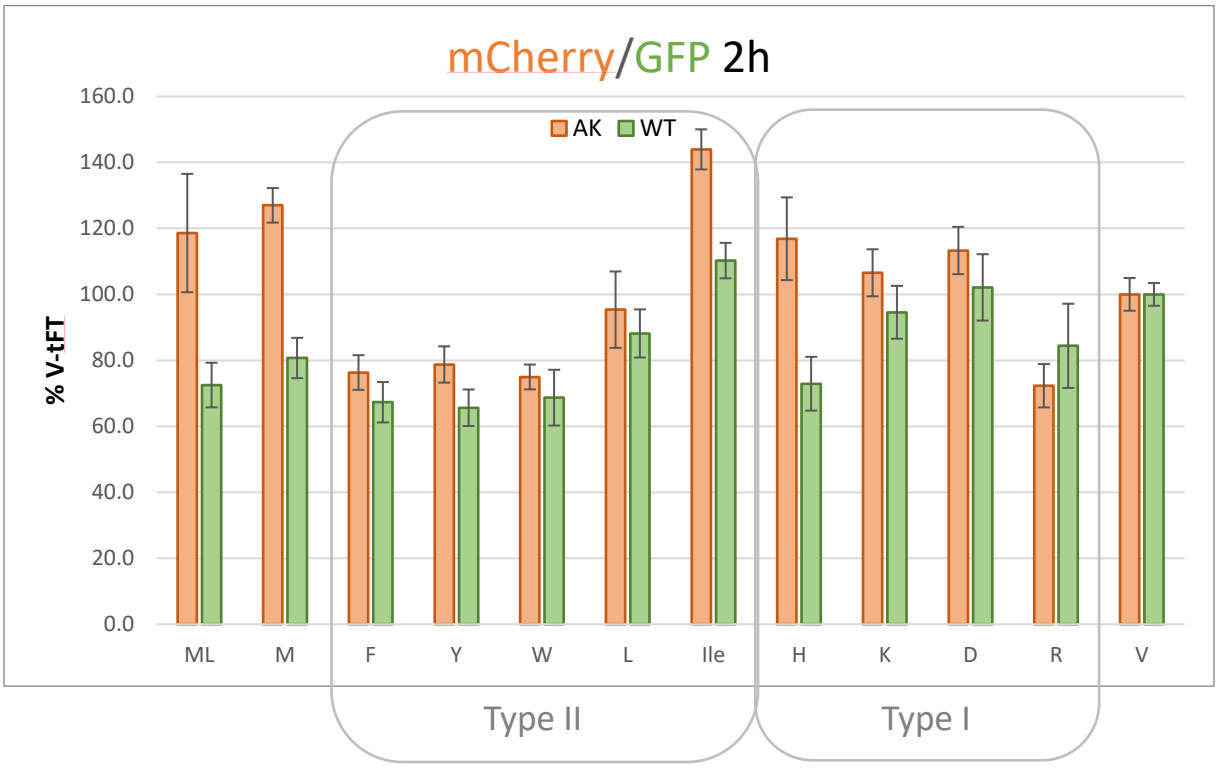

Figure 30: Bar plot for PRT6 double mutant AK (orange) compared to wild type (green), results for red/green fluorescence after 2 hours incubation, relative to V-tFT, set to 100%

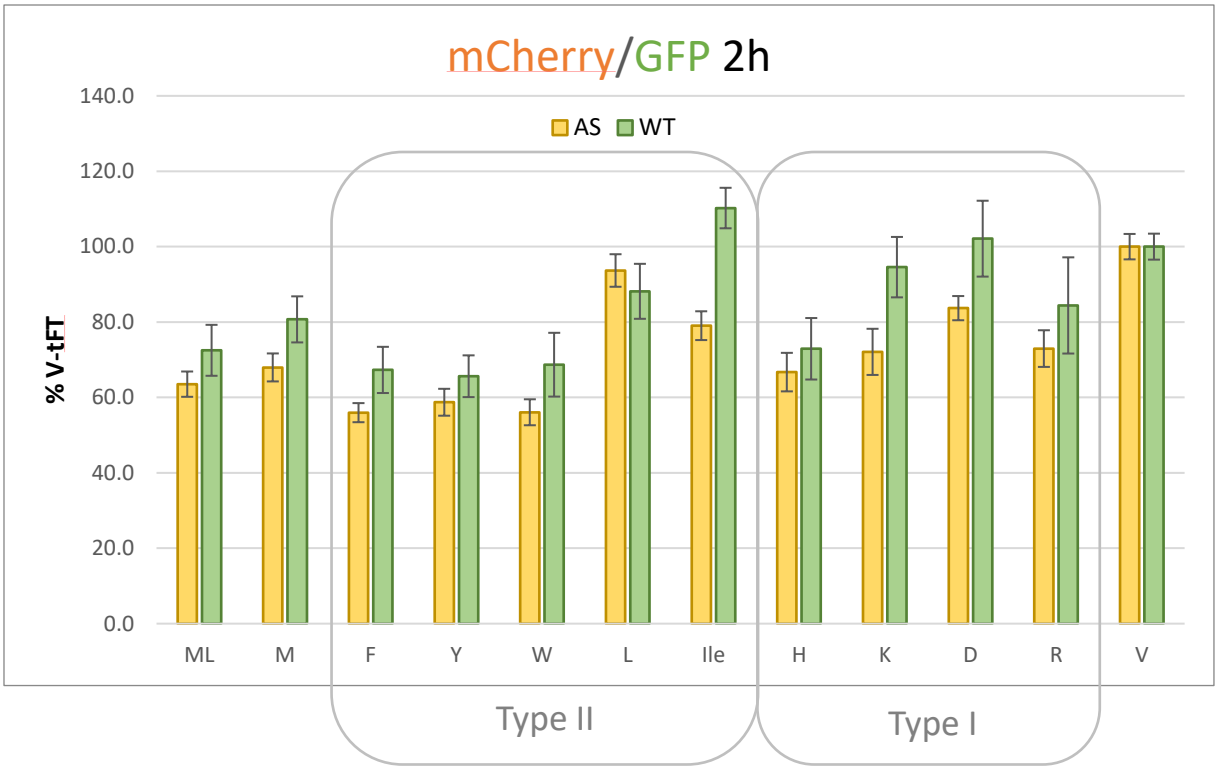

Figure 31: Bar plot for PRT6 double mutant AS (yellow) compared to wild type (green), results for red/green fluorescence after 2 hours incubation, relative to V-tFT, set to 100%

5.4.3 BIG

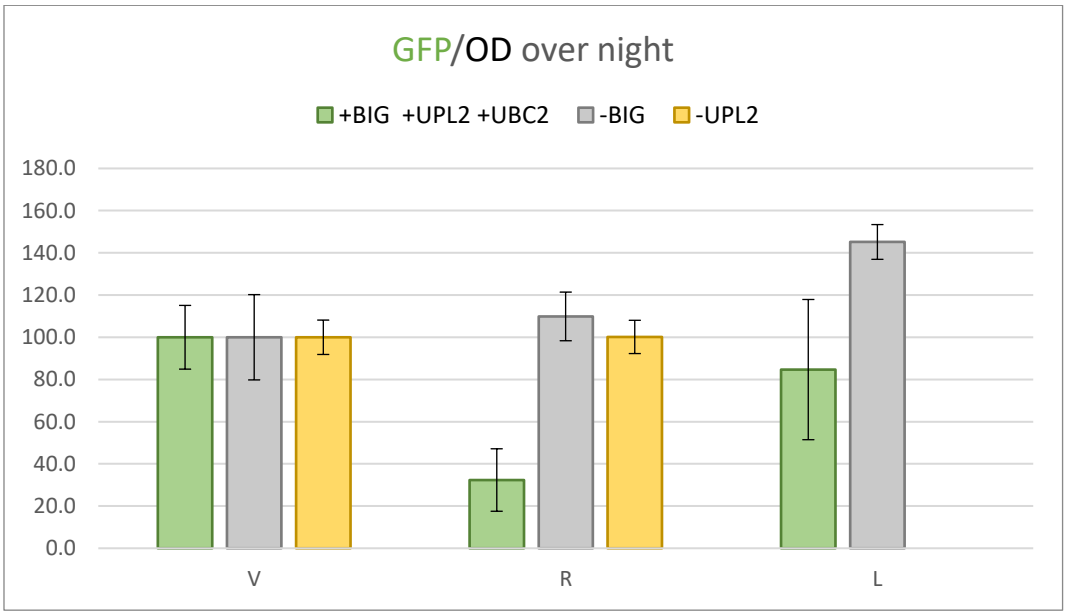

Figure 32: Bar plot for BIG + UPL2 + UBC2 (green), empty BIG vector + UPL2 +UBC2 (-BIG, grey) and BIG + empty UPL2 vector + UBC2 (-UPL2, yellow), data for GFP/OD$_{600}$ after overnight incubation, relative to V-tFT, set to 100%

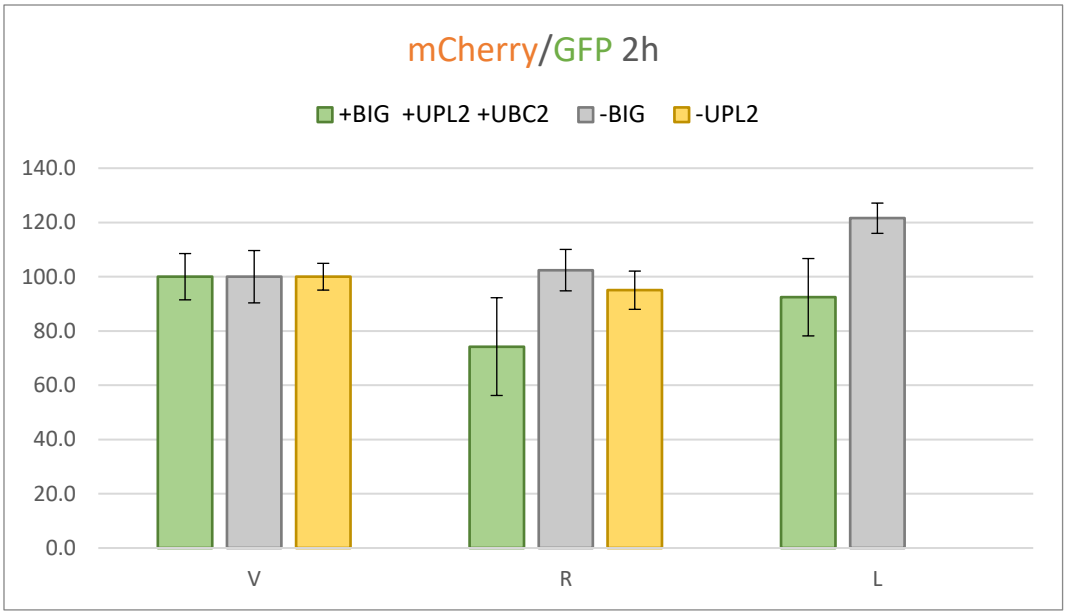

Figure 33: Bar plot for BIG + UPL2 + UBC2 (green), empty BIG vector + UPL2 +UBC2 (-BIG, grey) and BIG + empty UPL2 vector + UBC2 (-UPL2, yellow), data for red/green fluorescence after 2 hours incubation, relative to V-tFT, set to 100%

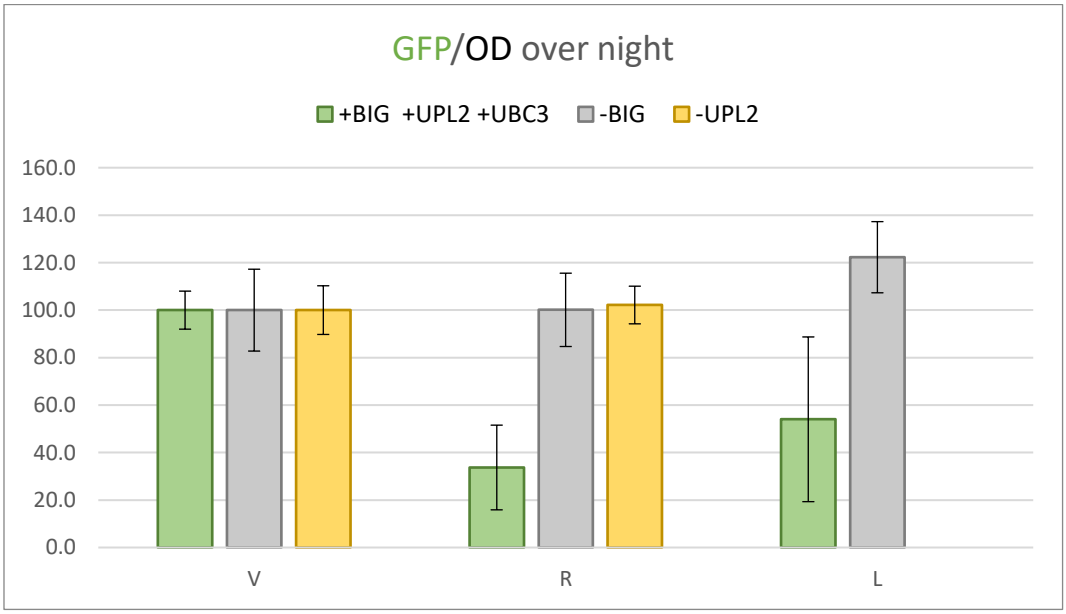

Figure 34: Bar plot for BIG + UPL2 + UBC3 (green), empty BIG vector + UPL2 +UBC3 (-BIG, grey) and BIG + empty UPL2 vector + UBC3 (-UPL2, yellow), data for GFP/OD$_{600}$ after overnight incubation, relative to V-tFT, set to 100%

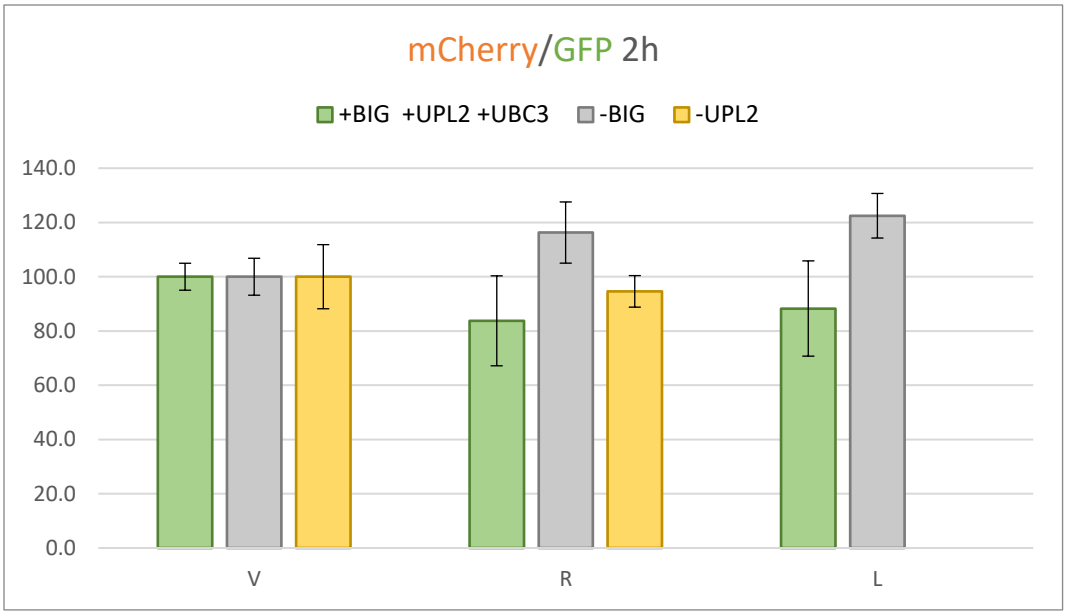

Figure 35: Bar plot for BIG + UPL2 + UBC3 (green), empty BIG vector + UPL2 +UBC3 (-BIG, grey) and BIG + empty UPL2 vector + UBC3 (-UPL2, yellow), data for red/green fluorescence after 2 hours incubation, relative to V-tFT, set to 100%

5.4.4 Infiltrations

48 hours after infiltration

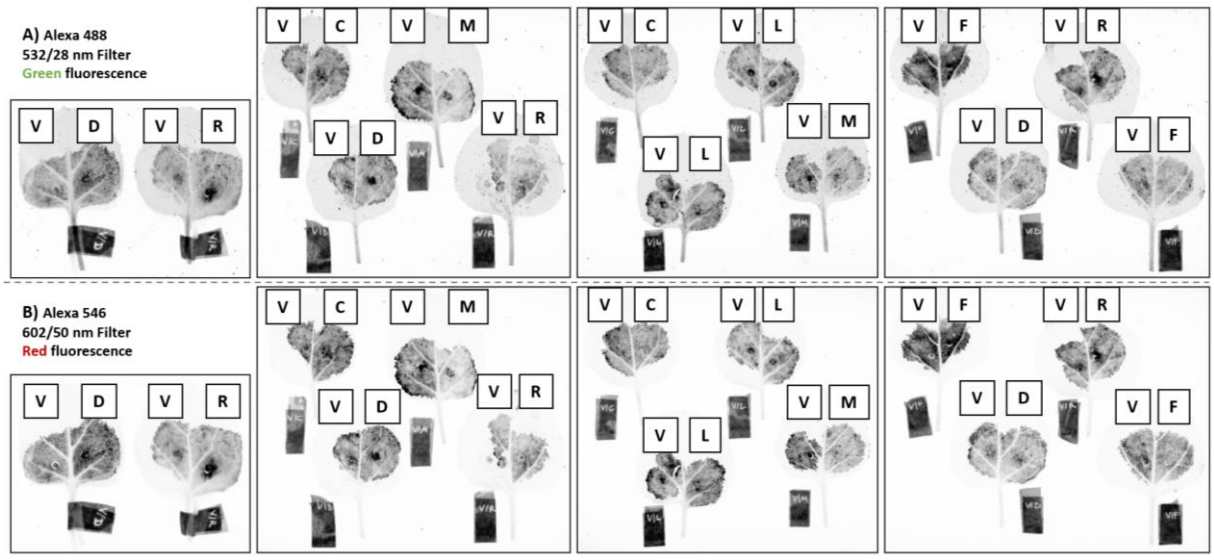

Figure 36: Further N. benthamiana infiltrations 48 hours after infiltration for green fluorescence (upper part) and red fluorescence (lower part)

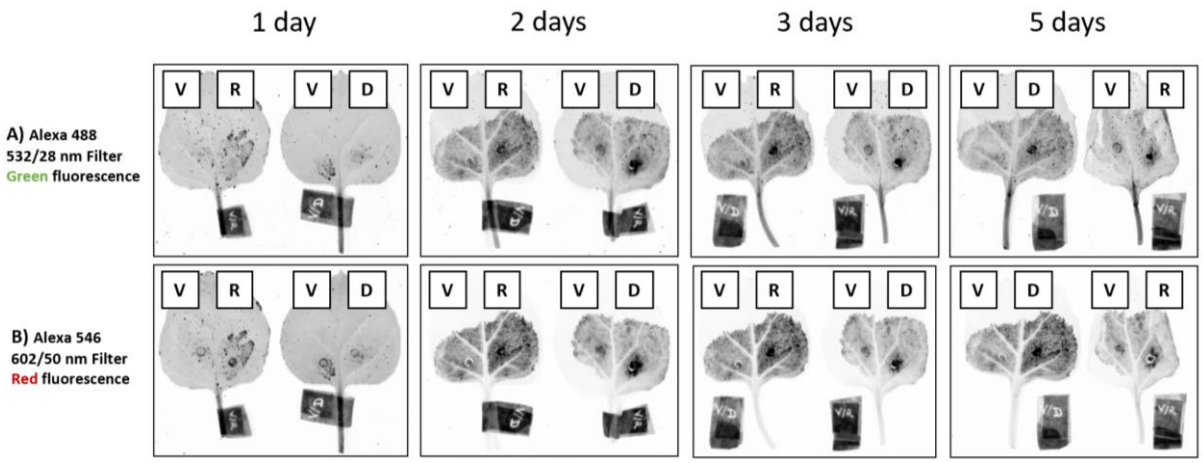

Figure 37: R- and D- compared to V-tFT over 5 days, green (upper part) and red (lower part) fluorescence

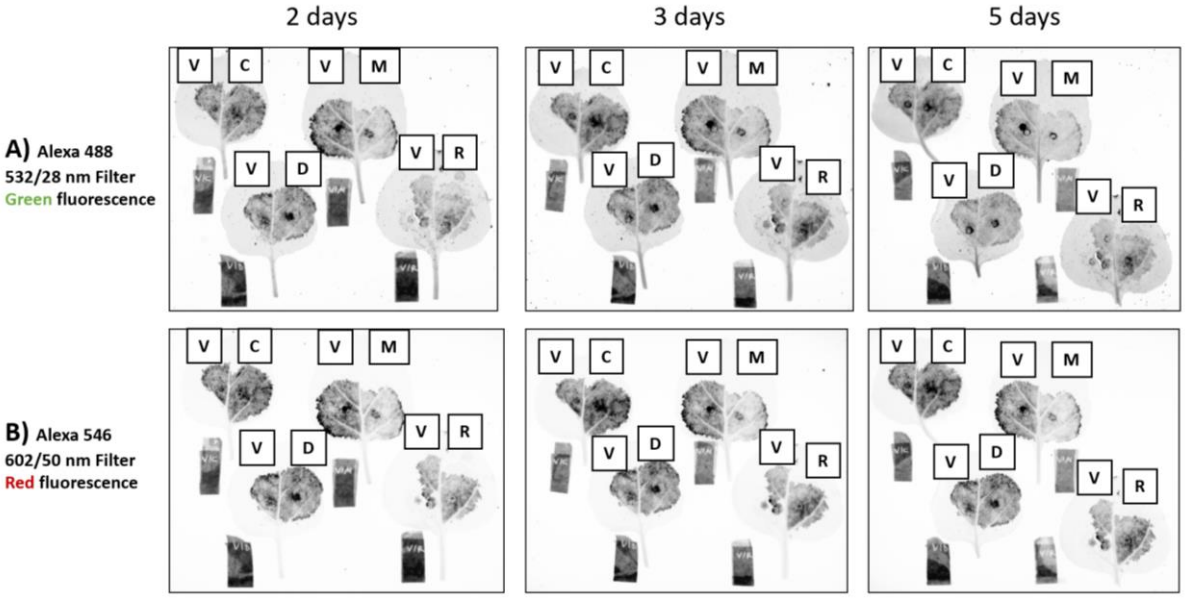

Figure 38: C-, M, R- and D- compared to V-tFT over 5 days, green (upper part) and red (lower part) fluorescence

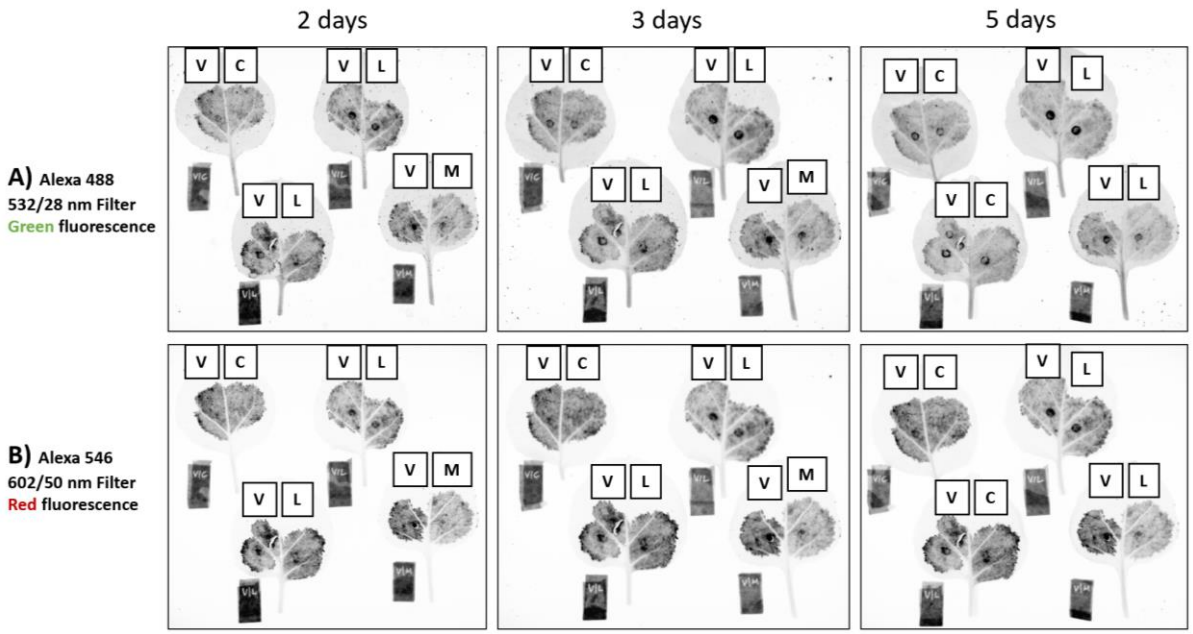

Figure 39: C-, L-, L- and M- compared to V-tFT over 5 days, green (upper part) and red (lower part) fluorescence

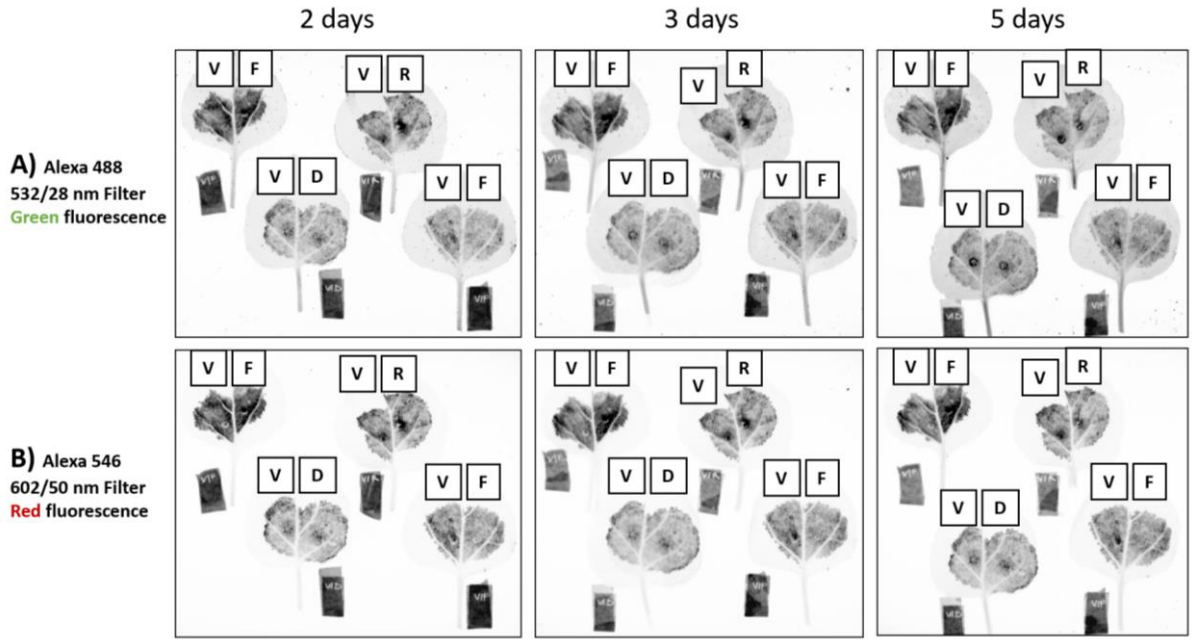

Figure 40: F-, R-, D- and F- compared to V-tFT over 5 days, green (upper part) and red (lower part) fluorescence

5.4.5 Plant Western Blots

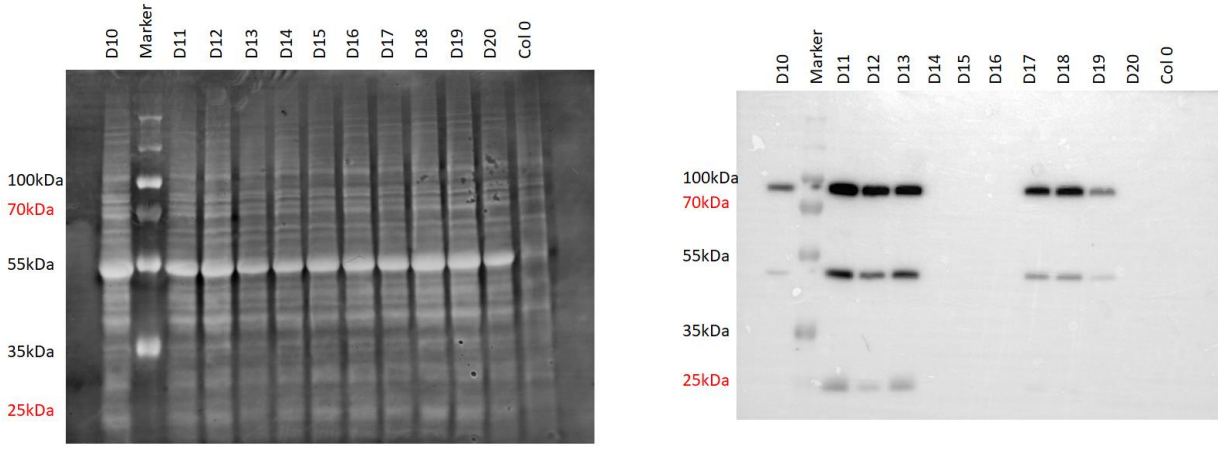

Figure 41: Further plant Western Blot 1, Ponceau stained (left side), and antibody labelled (right side)

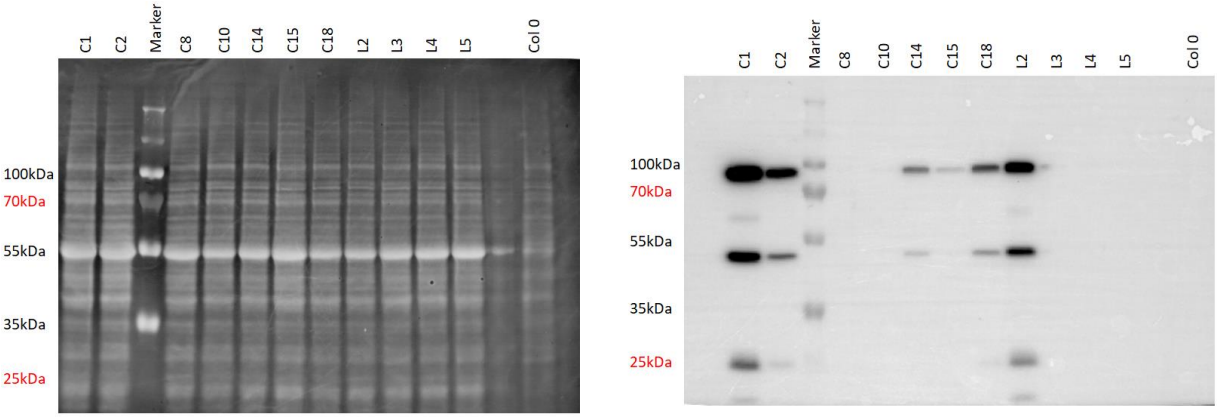

Figure 42: Further plant Western Blot 2, Ponceau stained (left side), and antibody labelled (right side)

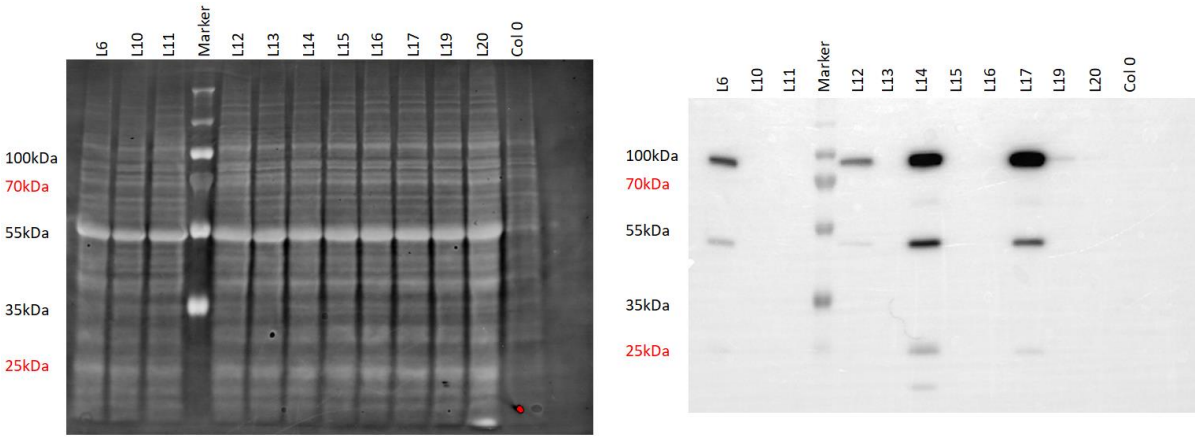

Figure 43: Further plant Western Blot 3, Ponceau stained (left side), and antibody labelled (right side)

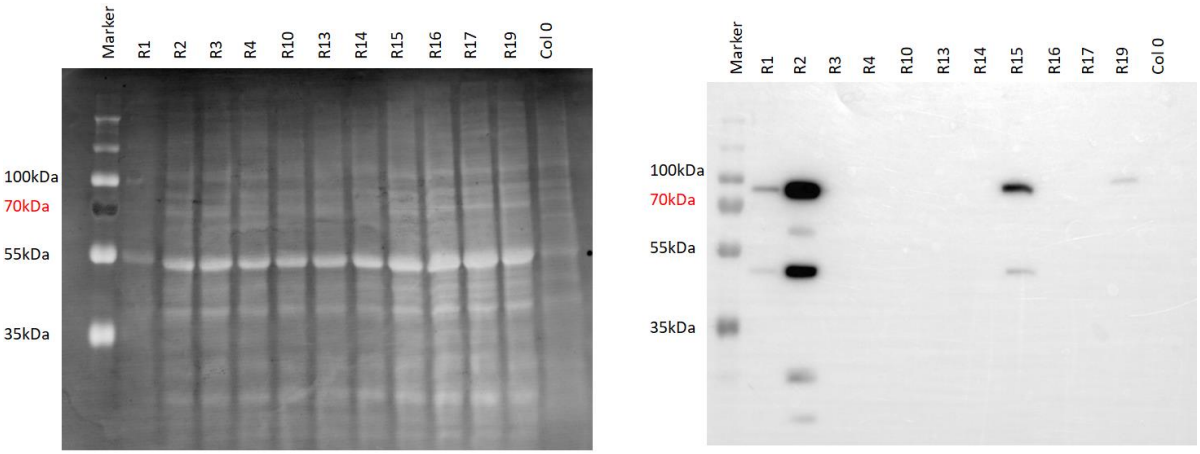

Figure 44: Further plant Western Blot 4, Ponceau stained (left side), and antibody labelled (right side)

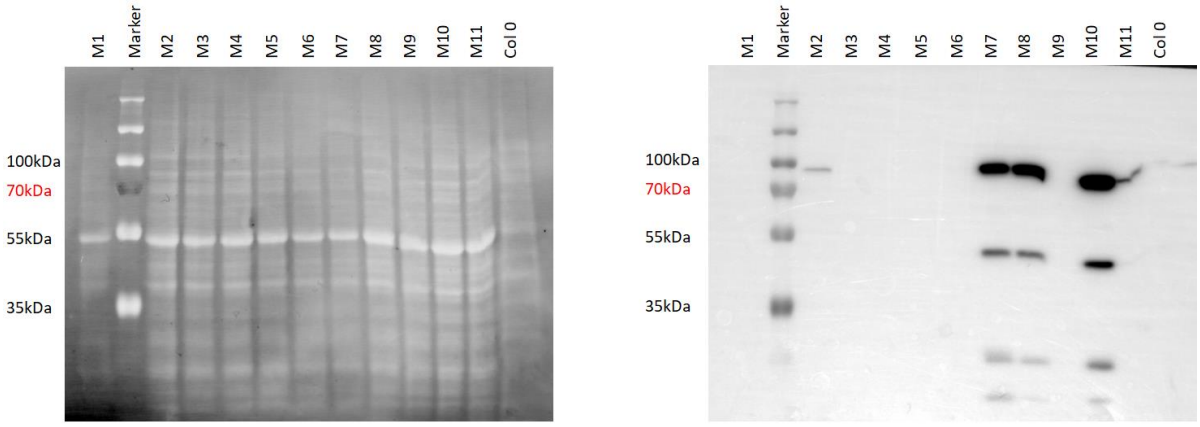

Figure 45: Further plant Western Blot 5, Ponceau stained (left side), and antibody labelled (right side)

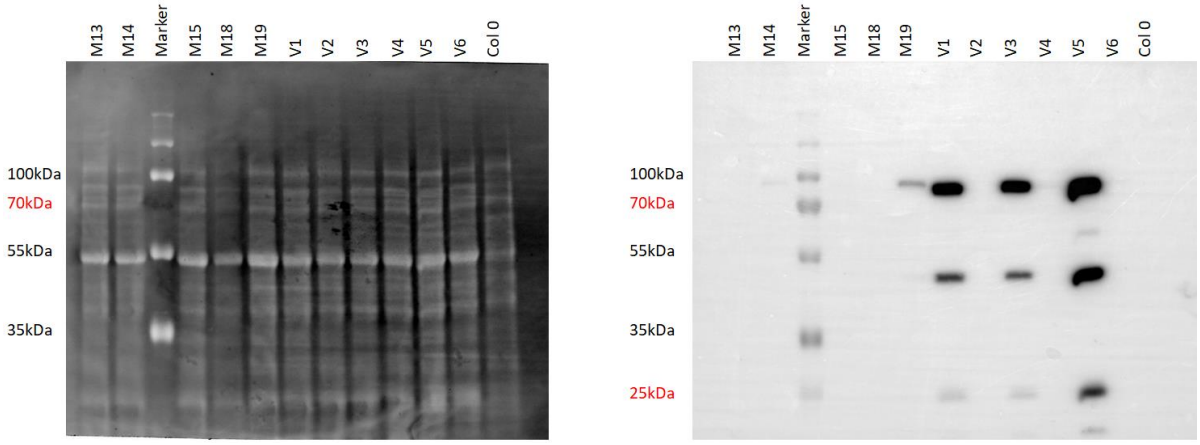

Figure 46: Further plant Western Blot 6, Ponceau stained (left side), and antibody labelled (right side)

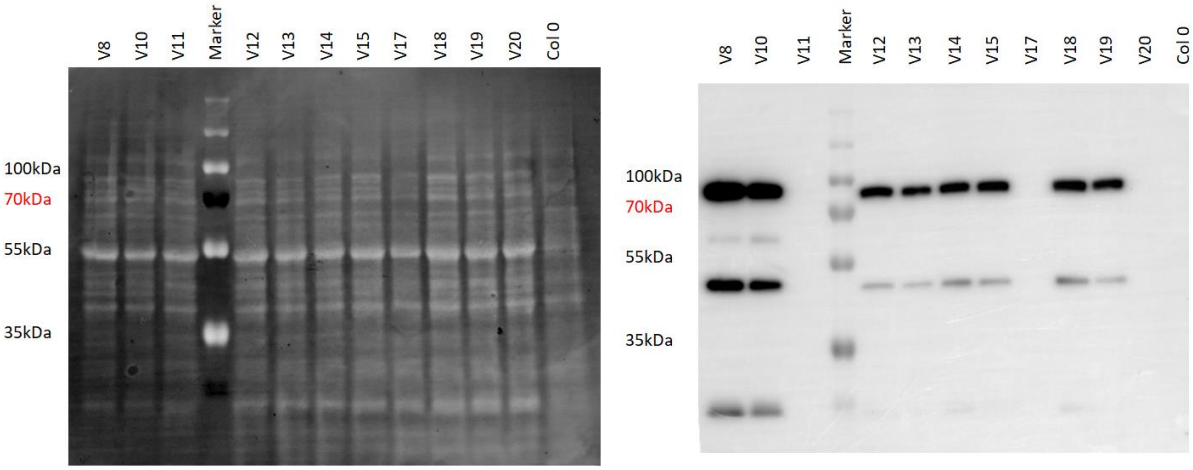

Figure 47: Further plant Western Blot 7, Ponceau stained (left side), and antibody labelled (right side)

6 References

Al-Saharin, Raed; Hellmann, Hanjo; Mooney, Sutton (2022): Plant E3 Ligases and Their Role in Abiotic Stress Response. In: *Cells* 11 (5). DOI: 10.3390/cells11050890.

Bachmair, Andreas; Becker, Frank; Schell, Jeff (1993): Use of a reporter transgene to generate Arabidopsis mutants in ubiquitin-dependent protein degradation. In: *Proceedings of the National Academy of Sciences of the United States of America* (90), S. 418–421.

Bachmair, Andreas; Finley, Daniel; Varshavsky, Alexander (1986): In Vivo Half-Life of a Protein Is a Function of Its Amino-Terminal Residue.

Bates, P. W.; Vierstra, R. D. (1999): UPL1 and 2, two 405 kDa ubiquitin-protein ligases from Arabidopsis thaliana related to the HECT-domain protein family. In: *The Plant journal : for cell and molecular biology* 20 (2), S. 183–195. DOI: 10.1046/j.1365-313x.1999.00590.x.

Böhm, Jessica; Winter, Nikola; Kozlic, Aida; Telser, Theresia; Nehlin, Lilian; Bachmair, Andreas (2023): Analysis of higher plant N-degron pathway components and substrates via expression in S. cerevisiae. In: *Methods in Enzymology* 686, S. 221–233. DOI: 10.1016/bs.mie.2023.02.006.

Chen, Liyuan; Hellmann, Hanjo (2013): Plant E3 ligases: flexible enzymes in a sessile world. In: *Molecular plant* 6 (5), S. 1388–1404. DOI: 10.1093/mp/sst005.

Clough, S. J.; Bent, A. F. (1998): Floral dip: a simplified method for Agrobacterium-mediated transformation of Arabidopsis thaliana. In: *The Plant journal : for cell and molecular biology* 16 (6), S. 735–743. DOI: 10.1046/j.1365-313x.1998.00343.x.

Dissmeyer, Nico (2019): Conditional Protein Function via N-Degron Pathway-Mediated Proteostasis in Stress Physiology. In: *Annual review of plant biology* 70, S. 83–117. DOI: 10.1146/annurev-arplant-050718-095937.

Garzón, Marcus; Eifler, Karolin; Faust, Andrea; Scheel, Hartmut; Hofmann, Kay; Koncz, Csaba et al. (2007): PRT6/At5g02310 encodes an Arabidopsis ubiquitin ligase of the N-end rule pathway with arginine specificity and is not the CER3 locus. In: *FEBS letters* 581 (17), S. 3189–3196. DOI: 10.1016/j.febslet.2007.06.005.

Generoso, Wesley Cardoso; Gottardi, Manuela; Oreb, Mislav; Boles, Eckhard (2016): Simplified CRISPR-Cas genome editing for Saccharomyces cerevisiae. In: *Journal of microbiological methods* 127, S. 203–205. DOI: 10.1016/j.mimet.2016.06.020.

Gibbs, Daniel J.; Bacardit, Jaume; Bachmair, Andreas; Holdsworth, Michael J. (2014): The eukaryotic N-end rule pathway: conserved mechanisms and diverse functions. In: *Trends in cell biology* 24 (10), S. 603–611. DOI: 10.1016/j.tcb.2014.05.001.

Gietz, Daniel R.; Sugino, Akio (1988): New yeast-Escherichia coli shuttle vectors constructed with in vitro mutagenized yeast genes lacking six-base pair restriction sites. In: *Elsevier* (74), S. 527–534.

Gietz, Daniel R.; Woods, Robin A. (2002): Transformation of Yeast by Lithium Acetate/Single-Stranded Carrier DNA/Polyethylene Glycol Method. In: *Methods in Enzymology* (350).

Heo, Ah Jung; Kim, Su Bin; Ji, Chang Hoon; Han, Dohyun; Lee, Su Jin; Lee, Su Hyun et al. (2021): The N-terminal cysteine is a dual sensor of oxygen and oxidative stress. In: *Proceedings of the National Academy of Sciences of the United States of America* 118 (50). DOI: 10.1073/pnas.2107993118.

Holdsworth, Michael John; Vicente, Jorge; Sharma, Gunjan; Abbas, Mohamad; Zubrycka, Agata (2020): The plant N-degron pathways of ubiquitin-mediated proteolysis. In: *Journal of integrative plant biology* 62 (1), S. 70–89. DOI: 10.1111/jipb.12882.

Hong, Jenny H.; Kaustov, Lilia; Coyaud, Etienne; Srikumar, Tharan; Wan, Janet; Arrowsmith, Cheryl; Raught, Brian (2015): KCMF1 (potassium channel modulatory factor 1) Links RAD6 to UBR4 (ubiquitin N-recognin domain-containing E3 ligase 4) and lysosome-mediated degradation. In: *Molecular & cellular proteomics : MCP* 14 (3), S. 674–685. DOI: 10.1074/mcp.M114.042168.

Khmelinskii, Anton; Keller, Philipp J.; Bartosik, Anna; Meurer, Matthias; Barry, Joseph D.; Mardin, Balca R. et al. (2012): Tandem fluorescent protein timers for in vivo analysis of protein dynamics. In: *Nature America*.

Kim, Jung Gi; Shin, Ho-Chul; Seo, Taewook; Nawale, Laxman; Han, Goeun; Kim, Bo Yeon et al. (2021): Signaling Pathways Regulated by UBR Box-Containing E3 Ligases. In: *International journal of molecular sciences* 22 (15). DOI: 10.3390/ijms22158323.

Kim, Leehyeon; Lin, Chih-Cheng; Lin, Ting-Jhen; Cao, Yan-Cih; Chen, Min-Chun; Chou, Mei-Yi et al. (2022): Structural analyses of the plant PRT6-UBR box in the Cys-Arg/N-degron pathway and insights into the plant submergence response: bioRxiv preprint 19.08.2022.

Kim, Sung Tae; Lee, Yoon Jee; Tasaki, Takafumi; Hwang, Joonsung; Kang, Min Jueng; Yi, Eugene C. et al. (2018): The N-recognin UBR4 of the N-end rule pathway is required for neurogenesis and homeostasis of cell surface proteins. In: *PloS one* 13 (8), e0202260. DOI: 10.1371/journal.pone.0202260.

Kozlic, Aida; Winter, Nikola; Telser, Theresia; Reimann, Jakob; Rose, Katrin; Nehlin, Lilian et al. (2021): A Yeast-Based Functional Assay to Study Plant N-Degron - N-Recognin Interactions. In: *Frontiers in plant science* 12, S. 806129. DOI: 10.3389/fpls.2021.806129.

Lorenz, Alexander (2015): New cassettes for single-step drug resistance and prototrophic marker switching in fission yeast. In: *Yeast (Chichester, England)* 32 (12), S. 703–710. DOI: 10.1002/yea.3097.

Meinke, David W.; Cherry, J. Michael; Dean, Caroline; Rounsley, Steven D.; Koornneef, Maarten (1998): Arabidopsis thaliana: A Model Plant for Genome Analysis.

Millar, A. Harvey; Heazlewood, Joshua L.; Giglione, Carmela; Holdsworth, Michael J.; Bachmair, Andreas; Schulze, Waltraud X. (2019): The Scope, Functions, and Dynamics of Posttranslational Protein Modifications. In: *Annual review of plant biology* 70, S. 119–151. DOI: 10.1146/annurev-arplant-050718-100211.

Modrego, Abelardo; Pasternak, Taras; Omary, Moutasem; Albacete, Alfonso; Cano, Antonio; Pérez-Pérez, José Manuel; Efroni, Idan (2023): Mapping of the Classical Mutation rosette Highlights a Role for Calcium in Wound-Induced Rooting. In: *Plant & cell physiology* 64 (2), S. 152–164. DOI: 10.1093/pcp/pcac163.

Mogk, Axel; Schmidt, Ronny; Bukau, Bernd (2007): The N-end rule pathway for regulated proteolysis: prokaryotic and eukaryotic strategies. In: *Trends in cell biology* 17 (4), S. 165–172. DOI: 10.1016/j.tcb.2007.02.001.

Pan, Man; Zheng, Qingyun; Wang, Tian; Liang, Lujun; Mao, Junxiong; Zuo, Chong et al. (2021): Structural insights into Ubr1-mediated N-degron polyubiquitination. In: *Nature* 600 (7888), S. 334–338. DOI: 10.1038/s41586-021-04097-8.

Pickart, Cecile M. (2001): Mechanisms Underlying Ubiquitination.

Sherpa, Dawafuti; Chrustowicz, Jakub; Schulman, Brenda A. (2022): How the ends signal the end: Regulation by E3 ubiquitin ligases recognizing protein termini. In: *Molecular cell* 82 (8), S. 1424–1438. DOI: 10.1016/j.molcel.2022.02.004.

Shu, Kai; Yang, Wenyu (2017): E3 Ubiquitin Ligases: Ubiquitous Actors in Plant Development and Abiotic Stress Responses. In: *Plant & cell physiology* 58 (9), S. 1461–1476. DOI: 10.1093/pcp/pcx071.

Stary, Susanne; Yin, Xiao-jun; Potuschak, Thomas; Schlögelhofer, Peter; Nizhynska, Victoria; Bachmair, Andreas (2003): PRT1 of Arabidopsis is a ubiquitin protein ligase of the plant N-end rule pathway with specificity for aromatic amino-terminal residues. In: *Plant physiology* 133 (3), S. 1360–1366. DOI: 10.1104/pp.103.029272.

Tasaki, Takafumi; Sriram, Shashikanth M.; Park, Kyong Soo; Kwon, Yong Tae (2012): The N-end rule pathway. In: *Annual review of biochemistry* 81, S. 261–289. DOI: 10.1146/annurev-biochem-051710-093308.

Toma-Fukai, Sachiko; Shimizu, Toshiyuki (2021): Structural Diversity of Ubiquitin E3 Ligase. In: *Molecules (Basel, Switzerland)* 26 (21). DOI: 10.3390/molecules26216682.

Varshavsky, Alexander (2011): The N-end rule pathway and regulation by proteolysis. In: *Protein science : a publication of the Protein Society* 20 (8), S. 1298–1345. DOI: 10.1002/pro.666.

Vierstra, Richard D. (2009): The ubiquitin-26S proteasome system at the nexus of plant biology. In: *Nature reviews. Molecular cell biology* 10 (6), S. 385–397. DOI: 10.1038/nrm2688.

Zhang, Hongtao; Rundle, Chelsea; Winter, Nikola; Miricescu, Alexandra; Mooney, Brian C.; Bachmair, Andreas et al. (2023): BIG participates in the Arg/N-degron pathways and the hypoxia response in Arabidopsis thaliana: bioRxiv preprint 27.05.2023.

Zheng, Ning; Shabek, Nitzan (2017): Ubiquitin Ligases: Structure, Function, and Regulation. In: *Annual review of biochemistry* 86, S. 129–157. DOI: 10.1146/annurev-biochem-060815-014922.

Zhu, Baogong; Cai, Guifang; Hall, Emily O.; Freeman, Gordon J. (2007): In-fusion assembly: seamless engineering of multidomain fusion proteins, modular vectors, and mutations. In: *BioTechniques* 43 (3), S. 354–359. DOI: 10.2144/000112536.